NeuroImage xxx (2010) xxx–xxx

Contents lists available at ScienceDirect

NeuroImage

journal homepage: www.elsevier.com/locate/ynimg

On a Gaussian neuronal field model

Wenlian Lu [a,*], Enrico Rossoni [b], Jianfeng Feng [a,b,*]

[a] Centre for Computational Systems Biology, Fudan University, Shanghai, PR China
[b] Centre for Scientific Computing, Warwick University, Coventry CV4 7AL, UK

ARTICLE INFO

Article history:
Received 28 July 2009
Revised 9 February 2010
Accepted 26 February 2010
Available online xxxx

ABSTRACT

Can we understand the dynamic behaviour of leaky integrate-and-fire (LIF) networks, which present the major, and possibly the only, analytically tractable tool we employ in computational neuroscience? To answer this question, here we present a theoretical framework on the spike activities of LIF networks by including the first order moment (mean firing rate) and the second order moment statistics (variance and correlation), based on a moment neuronal network (MNN) approach. The spike activity of a LIF network is approximated as a Gaussian random field and can reduce to the classical Wilson–Cowan–Amari (WCA) neural field if the variances vanish. Our analyses reveal several interesting phenomena of LIF networks. With a small clamped correlation and strong inhibition, the firing rate response function could be non-monotonic (not sigmoidal type), which can lead to interesting dynamics. For a feedforward and recurrent neuronal network, our setup allows us to prove that all neuronal spike activities rapidly synchronize, a well-known fact observed in both experiments and numerical simulations. We also present several examples of wave propagations in this field model. Finally, we test our MNN with the content-dependent working memory setting. The potential application of this random neuronal field idea to account for many experimental data is also discussed.

© 2010 Elsevier Inc. All rights reserved.

Introduction

Recent years have witnessed a significant growth in the field of biological computation (Dayan and Abbott, 2002; Destexhe and Contreras, 2006; Feng (editor), 2003). At this time, a closer unification between experimental and theoretical neuroscience has been observed. As a result, computational neuronal models emerge, owing more to their biological counterparts than previous classical artificially neural models. Voltage threshold models, such as the integrate-and-fire model (Lapicque, 1907), and the more biophysical Hodgkin–Huxley model (Hodgkin and Huxley, 1952), all incorporate more of the dynamics of actual biological neurons than the traditional classical approach to neural modelling.

In the literature, there are many papers analysing neuronal spiking dynamics based voltage threshold neuronal models. See Brette and Gerstner (2005), Brown et al. (1999), Buice and Chow (2007), Burak et al. (2009), Cai et al. (2004), Cateau and Reyes (2006), Fourcaud and Brunel (2002), Hildebrand et al. (2007), Jirsa (2004), Kovačič et al. (2009), Ly and Tranchina (2009), Memmesheimer and Timme (2006), Meyer and van Vreeswijk (2002), Pospischil et al. (2009), and Sporns (2003) and many others. As a basic approach, the input spike rates were approximated as a Gaussian process. Thus, Ornstein–Uhlenbeck (OU) processes were utilized to model the dynamics of membrane potentials. Some of them studied the dynamics/distribution of membrane potential, some studies concerned the firing rate (the first order moment) of the spikes, and some used modified IF neurons to investigate the spike activities. There are a number of papers (Ly and Tranchina, 2009 and others) considering the higher order moments in the LIF model. But, they have exclusively studied the moment properties of the ISI.

In addition, we have seen that there have been many attempts to use different random field models (Friston et al., 1994; Svensén et al., 2000; Pantazis et al., 2005; Wang and Rajapakse, 2006; Hayasaka et al., 2007; Caronell et al., 2009) to mimic and explain experimental data. Distinct from recent work (Harrison et al., 2005; Marreiros et al., 2009) concerned with probability density function (PDF) dynamics as well as the moment stochastic dynamics with respect to post-synaptic membrane depolarisation, capacitive current, and the time of last action potential, we focus on the spike activities of the neural ensemble, which is believed to be a significant functional signal in the brain.

Not surprisingly, attempting to describe neuronal network spike activities with partial differential equations (PDE) or field equations (FE) is a task that has been taken up by many authors (see for example, a recent excellent review by Deco et al. (2008)) and is still an active topic. A typical example of the classical approaches to modelling neuronal network activities is the well-known Wilson–Cowan–Amari (WCA) model (Wilson and Cowan, 1972, 1973; Amari, 1975,

* Corresponding authors. Feng is to be contacted at Centre for Computational Systems Biology, Fudan University, Shanghai, PR China.
E-mail addresses: wenlian.lu@gmail.com (W. Lu), jianfeng.feng@warwick.ac.uk (J. Feng).

1053-8119/$ – see front matter © 2010 Elsevier Inc. All rights reserved.
doi:10.1016/j.neuroimage.2010.02.075

1977), by which the firing rates of neural populations are described as follows:

$$\begin{cases} \tau_e \dfrac{\partial A_e(x,t)}{\partial t} = -A_e(x,t) + h_e\left(w_{ee}\left[W_{ee} * A_e(x,t)\right] - w_{ie}\left[W_{ie} * A_i(x,t)\right] + I_e(x,t)\right) \\ \tau_i \dfrac{\partial A_i(x,t)}{\partial t} = -A_i(x,t) + h_i\left(w_{ii}\left[W_{ii} * A_i(x,t)\right] - w_{ei}\left[W_{ei} * A_e(x,t)\right] + I_i(x,t)\right), \end{cases} \tag{1}$$

where e and i label the excitatory and inhibitory neurons respectively, $h_e(\cdot)$ and $h_i(\cdot)$ are activation (sigmoidal) functions, A_e, A_i are their firing rates, w_{ee}, w_{ei}, w_{ie}, and w_{ii} are the interaction strengths between them, W_{ee}, W_{ie}, W_{ei}, and W_{ii} are the normalized interaction structure between neurons of different types, I_e and I_i the external inputs to them, and τ_e, τ_i are two time constants, respectively. In this model, the membrane potential (the term inside h_e or h_i) is mapped into the firing rate, via sigmoidal functions. The model is widely used today with around ten citations per year from ISI web of knowledge and has been applied to simulate or mimic local field potentials (LFP), functional magnetic resonance imaging (fMRI), electroencephalogram (EEG), and magnetoencephalogram (MEG). See Erlhagen and Schöner (2002), and Griffith (1963, 1965) for examples. However, the properties of neuronal spikes can only be described by their firing rates. Computationally, if we intend to introduce, for example, the Bayesian approach in a neuronal network, we have to at least include the second order statistics such as the variance and the correlation in neuronal networks (Zhang et al., in press; Feng et al., 2004; Feng and Tuckwell, 2003). Hence, it is necessary to consider the dynamics of the second order moment statistics in a well-developed neural field model. So, the WCA model, despite succeeding many applications, cannot exactly match all aspects to biological meaningful quantities, as detailed in this paper.

Recently, we introduced a mathematical framework called *moment neuronal networks* (MNN) to link voltage threshold model to field model, described by the first and second order (or even higher) statistics of spike rates (Feng et al., 2007). Here, based on and continuing from the existing results, the purpose of this paper is to establish Gaussian random field model based on correlated OU processes to describe dynamics of neuronal spike trains. We study networks of correlated OU processes and establish evolution equations to describe dynamics of the first and second order statistics of the random point processes evoked by such correlated OU processes. We utilise these field equations, which in fact establishes a spatio-temporal Gaussian field (Vanmarke, 1983), to describe the dynamics of spike activities under several approximations. This model is named *Gaussian random neuronal field*. In comparison to Feng et al. (2007), in which the input–output correlation map is heuristically constructed and is simply the identical map, in this paper, the map is obtained using the linear perturbation theory (De La Rocha et al., 2007). Furthermore, only the mathematical properties of the MNN are simulated by Feng et al. (2007). In the current paper, we present some fundamental analytical results on the dynamics analysis of the Gaussian random neuronal field model and then apply the MNN framework in simple content-dependent working memory tasks.

As one would expect, when the variance in our model is removed, we can show that the continuous version of the MNN is reduced to the classical WCA model, because the firing rate function becomes sigmoidal. Interestingly, if we include the second moment in our model, there are essential differences between the continuous MNN and the WCA model. In the scenario where the inhibitory input is stronger than the excitatory, we obtain a non-monotonic firing rate response, similar to the tent or logistic map, which cannot be interpreted by the WCA model. Instead, as we are to show, this phenomenon is owing essentially to the second order statistics, i.e. coefficient of variance (CV). In addition, since CV is involved, in different reasonable physiological parameter region, the system has diverse fixed point attractors, including a deterministic firing train and a Poisson quasi-silent spiking. Besides, a more interesting phenomenon we obtain is a fixed point attractor of a low firing rate spontaneous activity, accompanied with the situation that the inhibitory input should be stronger than the excitatory input. Consequently, one can expect that the LIF network can exhibit very rich dynamic behaviours, including chaos, due to tent-like gain function.

Another advantage of the moment neuronal network approach over the classical mean firing rate approach is that it allows us to revisit synchronization phenomenon via this model. Biologically, synchronization between neuronal activities could play an essential role in neuronal computations and brain functions such as cognitions (Sarnthein et al., 1998), and attention selection (Varela et al., 2001; Niebur et al., 2002). Synchronization is surely a special case of correlated spike trains and the correlation is one of the second order statistics (Feng and Brown, 1999, 2000; Romo et al., 2004; De La Rocha et al., 2007). It has been earlier reported in the literature that a feedforward spiking network could easily lead to a stationary state of synchronized firing (Breakspear et al., 2003; Brunel and Wang, 2001; Miles et al., 1995; Reyes, 2003). The MNN framework allows us to theoretically prove that this is actually the case under specific conditions by the evolution equations of (Pearson) the correlation coefficients.

With correlations clamped, there are two variables of firing rate and variance, and so the description of a spike train can have more elaborate wave shapes in our model than the WCA model, even if just the wave propagation in the firing rate is considered. For example, we can construct a firing rate travelling wave in response to an input with almost zero firing rates but distinct variances in a local field. Moreover, we can construct a firing rate travelling wave with two bumps in response to an input with both distinct firing rate and variance distribution. As a further demonstration of the MNN approach, we then test the network performance in a content-dependent working memory task. Distinct from the well-known results in the literature where working memories are investigated in spiking neuronal networks independent of the content, the MNN approach allows us to tackle the issue within the framework of content-dependent working memories. Patterns can be stored and evoked in a MNN via both first- and second order moment statistics of the spike trains, using the simple Hebbian learning rule. Also, the limitations of this method are discussed.

Methods

In the theory of moment neuronal network (Feng et al., 2007), we represent (approximate) the spike activity of a neuron (a point process which is discrete) by a continuous process. For this purpose, the quantity we measure from the spike train is the density of spikes. In this section, we use this idea to establish the evolution equations for mean firing rates, variances, equivalently coefficients of variation, and correlation coefficients of an assembly of synaptically coupled neurons. This basic mathematical tool is an array of correlated OU processes and its first passage time theory (Tuckwell, 1988). To describe the spike rates of a LIF neuron by this way and derive their evolution equations, we need the following approximations:

- Renewal approximation: each spike train is regarded as a renewal process;
- Gaussian approximation: the number density of spike is approximated as Gaussianly distributed;
- Time-varying stationary approximation: the distribution of spike train at each time is approximated as stationary.

Thus, we can derive a map from the spike densities of the input to those of the output. With this map, since we treat the spike process as

Please cite this article as: Lu, W., et al., On a Gaussian neuronal field model, NeuroImage (2010), doi:10.1016/j.neuroimage.2010.02.075

time-varying stationary processes, we can model the neuronal activities as a Gaussian random field. This is the main idea of this paper.

Moment mapping

Consider a neuronal network with p neurons and model the potential activity of the i-th neuron as follows:

$$dV_i(t) = -LV_i(t)dt + \sum_j w_{ij}^E dN_j^{i,E}(t) + \sum_k w_{ik}^I dN_k^{i,I}(t), \tag{2}$$

where $1/L$ is the resistance, w_{ij}^E or w_{ik}^I is the EPSP and IPSP sizes from the j-th and k-th pre-synaptic neuron ($j, k = 1, 2, ..., p$) respectively, and $N_j^{i,E}(t)$ or $N_{jk}^{i,I}(t)$ is the input stimulus from the j-th or k-th pre-synaptic neurons, which is described a random point process. Since the discrete processes as defined by the right-hand side of Eq. (2) are usually difficult to be dealt with theoretically, here we approximate them by continuous processes. First, we regard the spike point process as the renewal processes:

$$dN_j^{i,v}(t) = \sum_k \delta\left(t - \sum_{l=1}^{k} T_{j,l}^{i,v}\right)dt,$$

with the l-th inter-spike interval (ISI) $T_{j,l}^{i,v}$ with $v = E$ or I. When $N_j^{i,v}(t)$ is a Poisson process, it has been extensively considered in many papers in the literature (Rieke et al., 1997; Leng et al., 2001; Gerstner and Kistler, 2002; Fourcaud et al., 2003). Since the number of renewals converges to a normal variable due to the central limit theorem, we have the following approximation for a sufficiently large t:

$$dN_j^{i,v}(t) \sim \mu_j^{i,v}dt + \sigma_j^{i,v}dB_j^{i,v}, \tag{3}$$

where $B_j^{i,v}, j = 1, ..., p$ are correlated Brownian motions. And, according to the renewal theorem (Cox and Lewis, 1996), the mean and variance of the number of renewals in a unit time interval are:

$$\mu_j^{i,v} = \frac{1}{T_{\text{ref}} + \langle T_{j,1}^{i,v}\rangle}, \quad \left(\sigma_j^{i,v}\right)^2 = \frac{\text{var}\left(T_{j,1}^{i,v}\right)}{\langle T_{\text{ref}} + T_{j,1}^{i,v}\rangle^3}, \tag{4}$$

where T_{ref} represents the refractory period and $\langle\cdot\rangle$ and $\text{var}(\cdot)$ denote the expectation and variance of a random variable, respectively.

Thus, Eq. (2) is approximated by correlated Ornstein–Uhlenbeck (OU) processes:

$$dV_i(t) = -LV_i(t)dt + \bar{\mu}_i dt + \bar{\sigma}_i dB_i(t), i = 1, ..., p, \tag{5}$$

where

$$\hat{\mu}_i = \sum_{j,v}\sum_{v=I,E} w_{ij}^v \mu_j^i, \quad \hat{\sigma}_i = \sqrt{\sum_{j,k}\sum_{v,u=I,E} w_{ij}^v \sigma_j^{i,v} \rho_{jk}^{i,v,u} w_{ik} \sigma_k^{i,u}}.$$

$\rho_{jk}^{i,v,u}$ is the correlation coefficient between the j-th and k-th synaptic inputs j and k to the neuron i, which is of type v and u, respectively. Initiated with a rest potential V_r, when the potential of the i-th neuron reaches a threshold V_{th}, the neuron emits a spike at that time and is rest back to V_r after a refractory period T_{ref}.

Then, from the LIF neuron model (5), we can establish a map from the first order and second order statistics of the input spiking trains to those of spiking trains. In terms of Siegert's expression (see Feng (editor), 2003), we can have the expression of all moments of the stationary inter-spike interval (ISI) distribution of the output spike trains. In particular, the mean and the variance of the output ISI can be written as:

$$\begin{aligned} \langle T_{\text{output},i}\rangle &= \frac{2}{L}\int_{I(V_r,\hat{\mu}_i,\hat{\sigma}_i)}^{I(V_{th},\hat{\mu}_i,\hat{\sigma}_i)} D_-(u)du \\ \text{Var}\left(T_{\text{output},i}\right) &= \frac{8}{L^2}\int_{I(V_r,\hat{\mu}_i,\hat{\sigma}_i)}^{I(V_{th},\hat{\mu}_i,\hat{\sigma}_i)} D_-\otimes D_-(u)du. \end{aligned} \tag{6}$$

Here,

$$I(\xi, y, z) = \frac{\xi L - y}{z},$$

$$D_-(u) = \exp\left(u^2\right)\int_{-\infty}^{u}\exp\left(-v^2\right)dv,$$

$$D_-\otimes D_-(u) = \exp\left(u^2\right)\int_{-\infty}^{u}\exp\left(-v^2\right)D_-^2(v)dv,$$

where $D_-(u)$ is exactly the Dawson's integral. For the details, we refer the interesting readers to Appendix C. We continue approximating the output spike trains as renewal processes. Using the renewal theory, we can obtain the mean and variance of the output spiking as

$$\mu_{\text{output},i} = \frac{1}{T_{\text{ref}} + \langle T_{\text{output},i}\rangle} = \frac{1}{T_{\text{ref}} + \frac{2}{L}\int_{I(V_r,\hat{\mu}_i,\hat{\sigma}_i)}^{I(V_{th},\hat{\mu}_i,\hat{\sigma}_i)} D_-(u)du},$$

$$\sigma_{\text{output},i} = \frac{\sqrt{Var\left(T_{\text{output},i}\right)}}{\left(\langle T_{\text{output},i}\rangle\right)^{3/2}} = \frac{\left(\frac{8}{L^2}\int_{I(V_r,\hat{\mu}_i,\hat{\sigma}_i)}^{I(V_{th},\hat{\mu}_i,\hat{\sigma}_i)} D_-\otimes D_-(u)du\right)^{1/2}}{\left(T_{\text{ref}} + \frac{2}{L}\int_{I(V_r,\hat{\mu}_i,\hat{\sigma}_i)}^{I(V_{th},\hat{\mu}_i,\hat{\sigma}_i)} D_-(u)du\right)^{3/2}}.$$

Let

$$S_1(y,z) \doteq \frac{1}{T_{\text{ref}} + \frac{2}{L}\int_{I(V_r,y,z)}^{I(V_{th},y,z)} D_-(u)du},$$

$$S_2(y,z) \doteq \frac{\left(\frac{8}{L^2}\int_{I(V_r,y,z)}^{I(V_{th},y,z)} D_-\otimes D_-(u)du\right)^{1/2}}{\left(T_{\text{ref}} + \frac{2}{L}\int_{I(V_r,y,z)}^{I(V_{th},y,z)} D_-(u)du\right)}.$$

In addition, we try to describe the map of correlation. There are diverse methods to define the correlation between point processes, basically, via the rates or timing. Here, we consider Pearson correlation coefficient of spike densities of neurons, which is defined by the correlation between the counts of two spiking trains in a sliding time windows. Let $L \gg 1$ be the full time length, T be the length time window, and Δt be the length of time bin. Define

$$y_i(t) = \begin{cases} 1 & \text{neuron i fires in } [t, t+\Delta t] \\ 0 & \text{otherwise} \end{cases}, \quad n_i(t) = \sum_{t'=t}^{t+T} y_i(t), t \in [0, L-T].$$

Define

$$\text{cov}\left(n_i, n_j\right) = \langle n_i(t), n_j(t)\rangle - \nu_i\nu_j.$$

Thus, the shift-correlation is defined as

$$\rho_T = \lim_{L\to\infty}\frac{\text{cov}(n_1 n_2)}{\sqrt{\text{Var}(n_1(t))\text{Var}(n_2(t))}}.$$

Thus, the correlation coefficient of spike strains is defined as its limit:

$$\rho = \lim_{T\to\infty}\rho_T.$$

Please cite this article as: Lu, W., et al., On a Gaussian neuronal field model, NeuroImage (2010), doi:10.1016/j.neuroimage.2010.02.075

It is clear that this definition of correlation coefficient coincides with that of Gaussian motions, which are used to describe spike processes after approximations. Also, the other is the cross-correlations, defined as:

$$C_{ij}(\tau) = \langle y_i(t) y_j(t+\tau)\rangle - \nu_i \nu_j$$

$$r_{12}(\Delta) = \frac{\int_{-\Delta}^{\Delta} C_{12}(\tau)d\tau}{\sqrt{\int_{-\Delta}^{\Delta} C_{11}(\tau)d\tau \int_{-\Delta}^{\Delta} C_{22}(\tau')d\tau'}}.$$

One can see that the coefficient of correlation between the output spike trains ρ_{out} satisfies $\rho_{\text{out}} = \lim_{\Delta\to\infty} r_{12}(\Delta) = \lim_{T\to\infty}\rho_T$. We note that it has been argued that the Pearson correlation coefficient has weakness to describe the correlation between neuronal spike activities, since it only consider the spike densities, which may artificially boost correlations (Amari and Nakahara, 2006; Averbeck et al., 2006).

Using the linear perturbation theory (De La Rocha et al., 2007; Lindner et al., 2005), we derive the map of the correlations from the input spike trains, $\rho_{\text{input}}(i, j)$, to those of the output, $\rho_{\text{output}}(i, j)$, as follows:

$$\rho_{\text{output}}(i,j) = \chi_{ij}\rho_{\text{input}}(i,j),$$

where $\rho_{\text{input}}(i, j)$, the correlation coefficient (CC) of the input spiking trains of the i-th and j-th neurons, has the form:

$$\rho_{\text{input}}(i,j) = \frac{(w_{i\cdot}\sigma_\cdot)^\top \sum (w_{j\cdot}\sigma_\cdot)}{\sqrt{(w_{i\cdot}\sigma_\cdot)^\top \sum (w_{i\cdot}\sigma_\cdot)}\sqrt{(w_{j\cdot}\sigma_\cdot)^\top \sum (w_{j\cdot}\sigma_\cdot)}},$$

and

$$\chi(i,j) = \frac{\hat\sigma_i\hat\sigma_j \frac{\partial S_1(\hat\mu_i,\hat\sigma_i)}{\partial \hat\mu_i}\frac{\partial S_1(\hat\mu_i,\hat\sigma_i)}{\partial \hat\mu_j}}{S_2(\hat\mu_i,\hat\sigma_i)S_2(\hat\mu_j,\hat\sigma_j)\sqrt{S_1(\hat\mu_i,\hat\sigma_i)S_1(\hat\mu_j,\hat\sigma_j)}}.$$

For more details about the expressions above, we refer interesting readers to Appendix A.

Thus, we are in the position to derive a map Γ, with respect to the means, variances, and correlations, from the input spiking trains to the output in the neuronal network as:

$$\begin{aligned}
&\Gamma : (\mu_{\text{input}}, \sigma_{\text{input}}, \Sigma_{\text{input}}) \to (\mu_{\text{output}}, \sigma_{\text{output}}, \Sigma_{\text{output}})\\
&\mu_{\text{output},\cdot} = S_1(\hat\mu_\cdot, \hat\sigma_\cdot)\\
&\sigma_{\text{output},\cdot} = S_2(\hat\mu_\cdot, \hat\sigma_\cdot)\sqrt{S_1(\hat\mu_\cdot, \hat\sigma_\cdot)}\\
&\rho_{\text{output},ij} = \begin{cases} \chi(i,j)\rho_{\text{input}}(i,j) & i\neq j\\ 1 & i=j.\end{cases}
\end{aligned} \tag{7}$$

Equivalently, sometimes in this paper, we can consider the coefficient of variation (CV) of the ISI, instead of the variance σ:

$$CV_i = \frac{\sqrt{\text{Var}(T_i)}}{\langle T_i\rangle} = \sqrt{\frac{\sigma_i^2}{\mu_i}}.$$

Thus, we have

$$CV_{\text{output},\cdot} = S_2(\hat\mu_\cdot, \hat\sigma_\cdot).$$

The moment neuronal network map can be described by three variables, (μ, σ, ρ), as depicted in Figs. 1A and B. In Fig. 1C, the relationship between input and output of the LIF model is plotted for $r = 0$, 0.5, 1, 1.5, 2 and $p = 100$. It is interesting that when $r > 1$, the firing rate response function bends like the tent or logistic map, in contrast to the well-known fact that it is always a sigmoidal function. However, in this scenario, we only peel one excitatory neuron from the population (the red one in Fig. 1C, right panel). For a more natural way to assess the activity of a single excitatory neuron, one can look at the neuron together with its environment (together with its surrounding inhibitory neurons), as the red neuron and its nearby inhibitory neurons marked by a circle in Fig. 1C, right panel.

Gaussian random neuronal field model

In previous section, we constructed a map from the input spiking point process to the output spiking point process by approximating them as renewal processes and Gaussian motions. Furthermore, we treat them as time-varying stationary processes. Using this Gaussian motion as the input for the next iteration, we can model the neuronal activities as a Gaussian field.

Evolution equations of the MNN: discrete-time and continuous-time models

We regard again the output of a LIF model as a renewal process (Humter, 1974) and Gaussian motions. So, these three classes of variables (firing rates, variances, and correlations) can fully describe the output Gaussian motions. Then, we derive evolution equations over these three classes of variables using the moment map. Thus, the spiking neuronal network is described by a Gaussian field.[1]

We now consider a Gaussian field of discrete time to model the underlying neuronal networks. We iterate the maps of moments to derive difference equations to describe the spike dynamics. Let $\mu(x, k)$ and $\sigma(x, k)$ the mean and variance at the location x of the k-th iteration if considering the feedforward neuronal network or the discrete time k if considering the recurrent neuronal network, and $\rho(x, y, k)$ the correlation between the location x and y at iteration k or time k. Let $w(x, y)$ be the interconnection coefficient between the locations x and y (sometimes it varies through time and then is denoted by $w(x, y, k)$). Define

$$\begin{aligned}
w * \mu(x,k) &= \int w(x,y)\mu(x,k)dy\\
\langle w*\sigma, w*\sigma\rangle\rho(k)(x,y,k) &= \int w(x,u)w(y,v)\sigma(u,k)\sigma(v,k)\rho(u,v,k)dudv.
\end{aligned}$$

Then, $\|w*\rho\|^2_{\rho(t)}(x,k) = \langle w*\sigma, w*\sigma\rangle_{\rho(t)}(x,x,k)$. Thus, the neuronal field yields the following iterative equations:

$$\begin{cases}
\mu(x,k+1) = S_1\left(w*\mu(x,k), \|w*\sigma\|_{\rho(k)}(x,k)\right)\\
\sigma(x,k+1) = S_2\left(w*\mu(x,k), \|w*\sigma\|_{\rho(k)}(x,k)\right) * \sqrt{S_1(w*\mu(x,k), \|w*\sigma\|\rho(k)(x,k))},\\
\rho(x,y,k+1) = \chi(x,y,k)\frac{\langle w*\sigma, w*\sigma\rangle_{\rho(k)}(x,y,k)}{\|w*\sigma\|_{\rho(k)}(x,k)\|w*\sigma\|_{\rho(k)}(y,k)}
\end{cases} \tag{8}$$

where $k = 1, 2, \cdots$, and

$$\chi(x,y,k) = \frac{\sigma(y,k)\sigma(x,k)\frac{d\mu}{d\hat\mu}(\hat\mu(x,k))\frac{d\mu}{d\hat\mu}(\hat\mu(y,k))}{S_2(x)S_2(y)\sqrt{S_1(x)S_1(y)}}.$$

Sometime, we consider the iterative equations of $CV(x, k)$, instead of σ, as follows:

$$CV(x,k+1) = S_2\left(w*\mu(x,k), \|w*\sigma\|_{\rho(k)}(x,k)\right).$$

[1] To construct a complete Gaussian random field, besides the means, variances, and the correlations, the map of auto-correlations should also be developed. However, we do not take them into considerations in this paper and will investigate them in the future work.

Please cite this article as: Lu, W., et al., On a Gaussian neuronal field model, NeuroImage (2010), doi:10.1016/j.neuroimage.2010.02.075

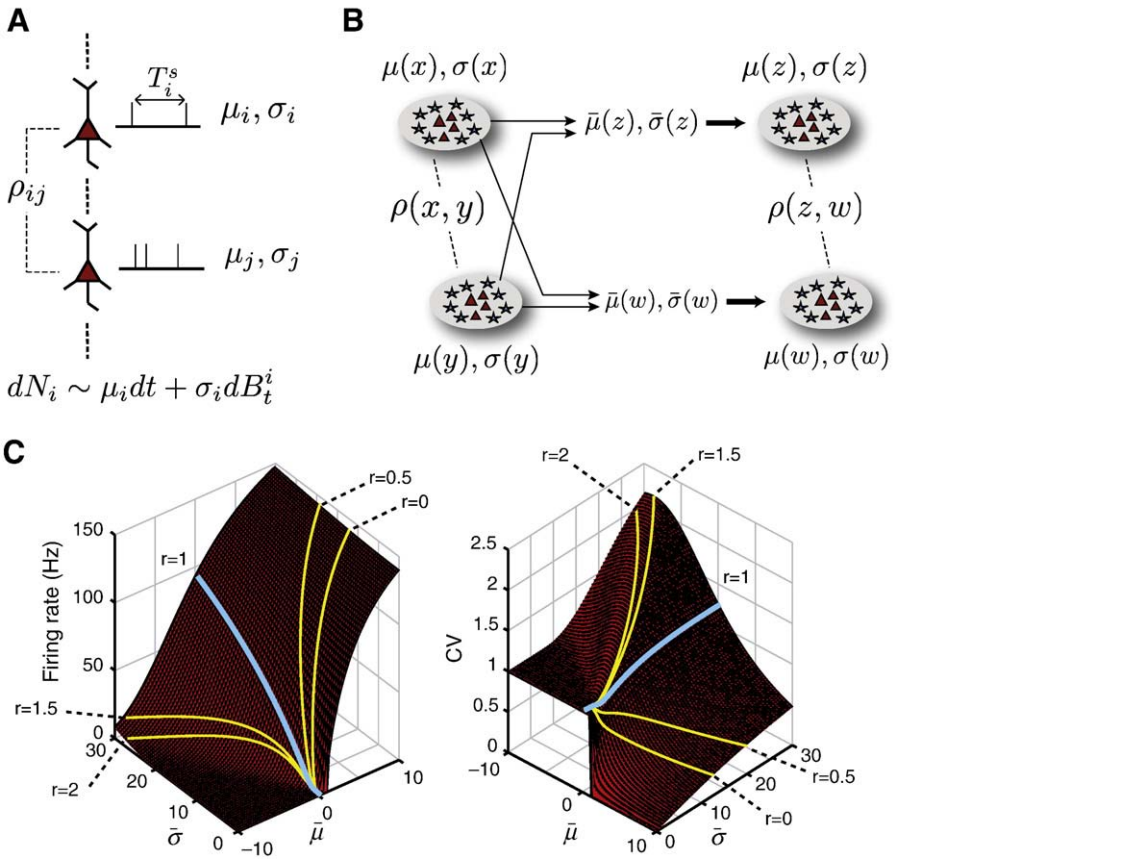

Fig. 1. Approximation described by Eq. (5) (A) and input–output relationship between output mean firing rate, CV and input $\overline{\mu}, \overline{\sigma}$ (B). In (B), right panel is the contour plot of CV (the middle one). In (A) and (B), trajectories indicated for are for $r = 0, 0.5, 1, 1.5, 2$, $\rho = 0.1$ and Poisson input case. (For interpretation of the references to color in this figure legend, the reader is referred to the web version of this article.)

In the continuous-time case, we can derive differential equations to describe their evolution directly from the map iterations. However, we use the moment maps for the stationary processes of the input and output spiking trains. So, when handling with the continuous-time model, we actually use a slow time scale such that the spike processes keep in a stationary state. Let t be continuous time which is much slower than that of the sampling. Thus, we can use the moment map to describe the dynamics of the moments of spike activities. Letting τ be the sampling time interval, the iterative Eq. (8) yields the following integro-differential equations:

$$\begin{cases} \tau \dfrac{\partial \mu}{\partial t} = -\mu + S_1\left(\omega * \mu, \|\omega * \sigma\|_\rho\right) \\ \tau \dfrac{\partial \sigma}{\partial t} = -\sigma + S_2\left(\omega * \mu, \|\omega * \sigma\|_\rho\right) \cdot \sqrt{S_1\left(\omega * \mu, \|\omega * \sigma\|_\rho\right)} \\ \tau \dfrac{\partial \rho}{\partial t} = -\rho + \chi_{x,y} \dfrac{\langle \omega * \sigma, \omega * \sigma \rangle_\rho}{\|\omega * \sigma\|_\rho(x) \|\omega * \sigma\|_\rho(y)} \end{cases} \tag{9}$$

where $t \in R$.

These maps can well approximate the dynamics of LIF neuron model. A lot of numerical illustrations are conducted in the literature. See Feng et al. (2007) and De La Rocha et al. (2007) for references. In the current paper, we present the dynamics analysis of the evolution equations we derive above.

For simplicity, in this paper, we assume that

$$w_{ij}^I = -r w_{ij}^E, \quad \sum = \{\rho(i,j)\} = \sum^E = \sum^I, \quad \mu_j = \mu_{j,1}^{i,E} = \mu_{j,1}^{i,I}, \quad \sigma_j = \sigma_{j,1}^{i,E} = \sigma_{j,1}^{i,I},$$

where r is the strength between inhibitory and excitatory input. $r = 1$ means that the input is exactly balanced, but $r > 1$ means that inhibitory input is stronger than excitatory input and the vice versa. Let

$$\overline{\mu}_i = \sum_{j=1}^{p} w_{ij} \mu_j, \overline{\sigma}_i = \sqrt{(w_{i\cdot}\sigma_\cdot)^\top \sum (w_{i\cdot}\sigma_\cdot)}.$$

Then, we have

$$\hat{\mu}_i = \overline{\mu}_i(1-r), \hat{\sigma}_i = \overline{\sigma}_i \sqrt{(1+r^2)}.$$

Comparison with WCA model

Consider an interesting case of Eq. (9) as $\sigma \to 0$. Clamped with a sufficiently small correlations $\rho(x, y)$, we study the stability of the following sub-manifold:

$$\mathcal{M} = \{(\mu, \sigma) : \sigma = 0\}.$$

For the spiking rate response function $S_1(\cdot,\cdot)$, we have the following algebras:

1. In case of $V_{th}L - (1-r)\overline{\mu} < 0$, the input is strong $\overline{\mu} > V_{th}L/(1-r)$ for $0 \le r < 1$. Repeating using the L'Hopstial's rule leads $D_-(x) \sim -\frac{1}{2x}$ as $x \to -\infty$. Since the remaining term is higher than $1/x$, we can see that

$$\lim_{\overline{\sigma} \to 0} \int_{\frac{V_r L - (1-r)\overline{\mu}}{\sqrt{L(1+r^2)}\overline{\sigma}}}^{\frac{V_{th}L - (1-r)\overline{\mu}}{\sqrt{(1+r^2)L}\overline{\sigma}}} D_-(u)du = \lim_{\overline{\sigma} \to 0} \int_{\frac{V_r L - (1-r)\overline{\mu}}{\sqrt{L(1+r^2)}\overline{\sigma}}}^{\frac{V_{th}L - (1-r)\overline{\mu}}{\sqrt{(1+r^2)L}\overline{\sigma}}} \left(-\frac{dx}{2x}\right)$$

$$= \ln \sqrt{\frac{(1-r)\overline{\mu} - V_r L}{(1-r)\overline{\mu} - V_{th}L}}.$$

Hence,

$$\lim_{\overline{\sigma}\to 0} S_1\left(\omega * \mu, \|\omega * \sigma\|_\rho\right) = \frac{1}{T_{\text{ref}} + \frac{2}{L}\ln\sqrt{\frac{(1-r)\overline{\mu}-V_r L}{(1-r)\overline{\mu}-V_{th}L}}}.$$

2. For $V_{th}L-(1-r)\overline{\mu}\geq 0$, since

$$\lim_{\overline{\sigma}\to 0}\int_{\frac{V_r L-(1-r)\overline{\mu}}{\sqrt{1+r^2}\overline{\sigma}}}^{\frac{V_{th}L-(1-r)\overline{\mu}}{\sqrt{1+r^2}\overline{\sigma}}} D_-(u)du = \infty,$$

we have $\lim_{\overline{\sigma}\to 0} S_1\left(\omega * \mu, \|\omega * \sigma\|_\rho\right) = 0$.

Then, we consider the variational equation of the variance σ, near $\sigma=0$. Let

$$A = \frac{8}{L^2}\int_{I\left(V_r,(1-r)\overline{\mu},\sqrt{1+r^2}\overline{\sigma}\right)}^{I\left(V_{th},(1-r)\overline{\mu},\sqrt{1+r^2}\overline{\sigma}\right)} \exp\left(u^2\right)du\int_{-\infty}^{u}\exp\left(-v^2\right)D_-^2(v)dv,$$

$$B = T_{\text{ref}} + \frac{2}{L}\int_{I\left(0,(1-r)\overline{\mu},\sqrt{1+r^2}\overline{\sigma}\right)}^{I\left(V_{th},(1-r)\overline{\mu},\sqrt{1+r^2}\overline{\sigma}\right)} D_-(u)du.$$

1. In case of $V_{th}L-(1-r)\overline{\mu}<0$, some algebra leads

$$A\sim\frac{\left(1+r^2\right)\overline{\sigma}^2}{2L}\left[\frac{1}{(V_{th}L-(1-r)\overline{\mu})^2}-\frac{1}{(V_r L-(1-r)\overline{\mu})^2}\right], \overline{\sigma}\to 0.$$

This implies

$$S_2\sqrt{S_1}\sim\kappa\overline{\sigma}, \text{ as } \overline{\sigma}\to 0,$$

with

$$\kappa = \frac{\sqrt{1+r^2}}{\sqrt{2L}\left(T_{\text{ref}}+\frac{2}{L}\ln\sqrt{\frac{(1-r)\overline{\mu}-V_r L}{(1-r)\overline{\mu}-V_{th}L}}\right)^{3/2}}\sqrt{\frac{1}{(V_r L-(1-r)\overline{\mu})^2}-\frac{1}{(V_{th}L-(1-r)\overline{\mu})^2}}.$$

Then, the variational equation of the variance becomes

$$\tau\dot{\sigma} = -\sigma + \kappa\overline{\sigma}.$$

Denote a candidate Lyapunov function as $V(\sigma)=\int\sigma^2(x)dx$ and differentiate it as

$$\begin{aligned}\dot{V}(\sigma) &= \frac{1}{\tau}\int dx\left(-2\sigma^2+2\kappa\sigma\overline{\sigma}\right)\\ &\leq\frac{1}{\tau}\int dx\left[-\sigma^2+\kappa^2\int w(x,u)w(x,v)\rho_{u,v}\sigma(u)\sigma(v)dudv\right].\end{aligned} \tag{10}$$

Let $f(u,v)=\int dx w(x,u)w(x,v)\rho_{u,v}$ and denote a quasi-linear operator by $F[\sigma]=\int f(u,v)\sigma(u)\sigma(v)dudv$. If $\kappa^2\|F\|_2<1$, we have the right-hand side in Ineq. (10) that is negative definite. This implies that $\lim_{t\to\infty}\sigma=0$. For instance, let $g(u,v)=\int dx|w(x,u)w(x,v)|$ and $G[\sigma]=\int g(u,v)\sigma(u)\sigma(v)dudv$. If the correlation $|\rho_{u,v}|<\rho_0$ with

$$\rho_0<\frac{1}{\kappa^2\|G\|_2}, \tag{11}$$

then we can conclude that $\sigma=0$ is asymptotically stable.

2. In case of $V_{th}L-(1-r)\overline{\mu}>0$, one can conclude $\lim_{\overline{\sigma}\to 0}\frac{1}{\overline{\sigma}}\left(S_2\sqrt{S_1}\right)=0$ via a long complicated algebras. This implies that the evolution equation upon the variance asymptotically becomes

$$\tau\dot{\sigma} = -\sigma.$$

So, $\sigma=0$ is clearly asymptotically stable.

Integrating the results above, we have

Theorem 2.2.1. *In both situations (the first case with sufficiently small correlations), the subspace $\mathcal{M}=\{(\mu,\sigma):\sigma=0\}$ is asymptotically stable and system (9) asymptotically approaches the following differential equation:*

$$\begin{cases}\tau\cdot\dfrac{\partial\mu}{\partial t} = -\mu+\mathcal{L}(\omega*\mu)\\ \sigma = 0,\end{cases} \tag{12}$$

where the firing rate response function $\mathcal{L}(\cdot)$ is a sigmoid-type function:

$$\mathcal{L}(v) = \begin{cases}\dfrac{1}{T_{\text{ref}}+\frac{2}{L}\ln\sqrt{\frac{(1-r)v-V_r L}{(1-r)v-V_{th}L}}} & v>V_{th}L/(1-r)\\ 0 & 0<v<V_{th}L/(1-r).\end{cases} \tag{13}$$

Under this condition as mentioned in this theorem, the continuous-time model approaches the WCA Eq. (1) since the firing rate function becomes sigmoidal. In this sense, as we have pointed out in the beginning of this paper, the WCA equation can be regarded as a special case of our moment neuronal network.

Results

In this section, we study the dynamical behaviour of the MNN model. We consider the discrete-time model (8) and continuous-time model (9) respectively and mainly focus on the differences from our model to the WCA model. Since the model is rather complicated to investigate, we make simplifications to conduct mathematical analysis. In discussion of the stable fixed points and the monotonicity of the firing rate response function, we fix the correlation and assume the weights of neuronal network are homogenous, when discussing the correlation, we fix the firing rate and variances, and use Heaviside functions to simplify the firing rate and variance response functions to design static travelling waves.

Stable low firing rate or low CV point attractors

Despite the approximation capability of the moment network to well-known WCA model, nonzero variances make much differences from the first order moment field model. For instance, in the WCA model, one can see that sufficiently small interconnections can lead that the network has

Please cite this article as: Lu, W., et al., On a Gaussian neuronal field model, NeuroImage (2010), doi:10.1016/j.neuroimage.2010.02.075

low firing rates, i.e., the field equations have an attractor with very low firing rates. In mathematics, we consider the following WCA model without external inputs:

$$\tau\frac{\partial A(x,t)}{\partial t} = -A(x,t) + \mathcal{L}\Big(\int w(x,y)A(y,t)dy\Big). \tag{14}$$

Since the firing rate response function $\mathcal{L}(\cdot)$ is a sigmoid function, which implies that $\lim_{\rho\to 0+}\ \mathcal{L}'(\rho) = 0$, one can see that the origin state: $A(x) = 0$ for all x, is asymptotically stable. That is, if the initial firing rates are very low and there are no external stimulus, the whole network can be trapped in the silent state (no spiking). At the same time, the variance keeps zero since it is a first order moment equation.

However, when the variance exists, there is a positive probability to emit spikes with certain firing rate even if the input firing rate is very low. Here, in order to mathematical reasoning, we male some simplifications by clamping the correlations as $\rho(x,y) = \rho$ for all $x \neq y$ and the same type of neurons, but equal to zero for different types of neurons, and setting uniform weights $w(x, y)$ for all x, y such that

$$\int w(x,y)dy = p$$

holds for all x. Thus, Eqs. (8) and (9) become homogenous:

$$\begin{cases} \mu(k+1) = S_1(\hat{\mu}(k), \hat{\sigma}(k)) \\ CV(k+1) = S_2(\hat{\mu}(k), \hat{\sigma}(k)), \end{cases} \tag{15}$$

with $CV(k) = \dfrac{\sigma(k)}{\sqrt{\mu(k)}}$, where $\hat{\mu}(k) = (1-r)p\mu(k)$ and $\hat{\sigma}(k) = \sqrt{(1+r^2)(p+p(p-1)\rho)}\sigma(k)$. Similarly, the continuous-time model can be written as

$$\begin{cases} \tau\dot{\mu} = -\mu + S_1(\hat{\mu}(k), \hat{\sigma}(k)) \\ \tau\dot{CV} = -CV + S_2(\hat{\mu}(k), \hat{\sigma}(k)). \end{cases} \tag{16}$$

The large deviation of Freidlin and Wentzell (1998) tells us that if $p\mu(0)(1-r) < V_{th}L$ and $\sigma(0)$ is small enough, the output of the system converges to a Poisson process asymptotically, i.e. the CV of the output converges to 1. Since the slope of firing rate response function is very low near zero, the firing rate will converge to silence: $\mu = 0$. So, the fixed point (0, 1) will be a stable fixed point of the neuronal field. In contrast, if $p\mu(0)(1-r) > V_{th}L$ and the $\sigma(0)$ is sufficiently small, the output becomes deterministic asymptotically, which implies $CV = 0$. In this situation, the neuron surly has nonzero firing rate and now the neuronal field Eq. (16) converges to WCA model. So, its stable fixed point is the nonzero solution of the equation $\mu = \mathcal{L}(p(1-r)\mu)$, which is stable in the asymptotical WCA equation, denoted by μ^*. Hence $(\mu^*, 0)$ is a stable fixed point. It is not difficult to see that in both scenarios, (0, 0) cannot be a stable fixed point, in contrast to the WCA model.

By Figs. 2 and 3, the theoretical analysis above is verified by simulating the Eq. (16). In Fig. 2, we simulate the propagation of activity in a homogeneous feedforward neuronal field and we take $p = 100$. As we expect, there are only two stable states (0, 1) and $(\mu^*, 0)$. The critical point of r is determined by the equation

$$\mu(1-r)p = V_{th}L$$

with $V_{th} = 20$ and $L = 1/20$. Hence for the dashed line, it is given by $r_c = 0.2$ for $\mu(0) = 50$, for the solid line it is $r_c = 0.1$ for $\mu(0) = 100$. It is clearly seen that the theoretical analysis above accurately describes the dynamical behaviours.

In Fig. 3A, we plot the stable fixed point attractors of the model with $p = 1000, \rho(i,j) = 0.003, i \neq j$. The red line is stable and blue is not. In general, we have three fixed points in the firing rate (see Fig. 3C, rate vs. r, the top trace). Here, we do not plot the trivial one, the quiet state. The upper branch corresponds to the highest firing rate state. When r is small, the firing rate is very high, above 100 Hz. There is a transition point at around 80 Hz where the stimulus changes from supthreshold to subthreshold. The upper branch and the middle branch lost their stability when r is sufficiently large.

Non-sigmoid firing rate response function

When $r > 1$, which implies that the inhibition is stronger than the excitation, our filed model indicates difference from the WCA model. One of most interesting points is that we can obtain a non-monotonic firing rate response according to the input. We study this phenomenon by analytically discussing our field model. First, we will analyze the monotonicity of the firing rate response function $S_1(\cdot,\cdot)$ with a fixed CV. Second, we will evolve the field equation to look into its dynamics of firing rate and CV with a fixed correlation.

Due to nonzero variance σ, the firing rate response function $S_1(\mu, \sigma)$ is no longer sigmoidal, even or monotonic in the case of $r > 1$. Recall the firing rate response function in the homogeneous MNN map Γ:

$$S_1(\mu,\sigma) = \frac{1}{T_{\text{ref}} + \frac{2}{L}\int_{I(V_r,\mu,\sigma)}^{I(V_{th},\mu,\sigma)} D_-(u)du}. \tag{17}$$

With a fixed $CV > 0$ and a common correlation coefficients (CC) ρ, its monotonicity is inverse to that of the following function

$$f(\mu) = \int_{\frac{V_rL-(1-r)\mu}{\sqrt{(1+r^2)(p+(p-1)p\rho)}\sigma}}^{\frac{V_{th}L-p(1-r)\mu}{\sqrt{(1+r^2)(p+(p-1)p\rho)}\sigma}} \exp\left(u^2\right)du \int_{-\infty}^{u} \exp\left(-v^2\right)dv.$$

Please cite this article as: Lu, W., et al., On a Gaussian neuronal field model, NeuroImage (2010), doi:10.1016/j.neuroimage.2010.02.075

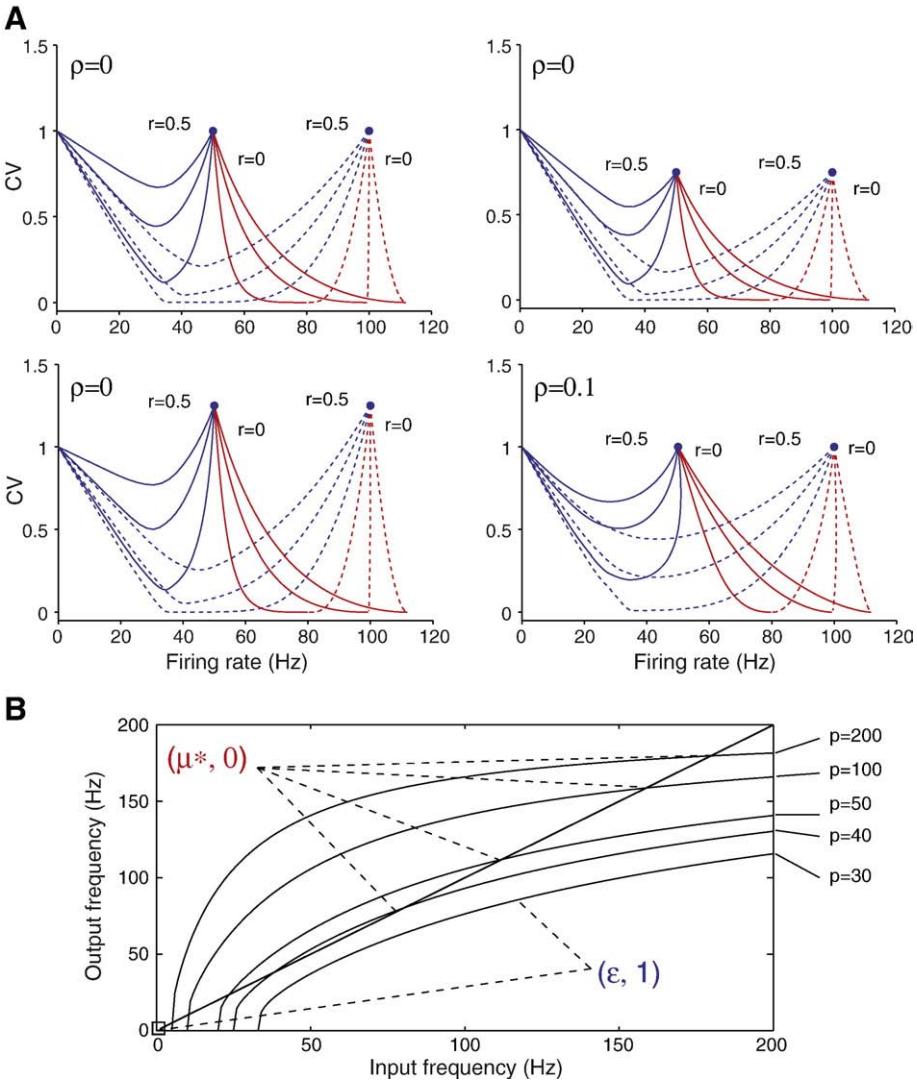

Fig. 2. Dynamics of the trajectories of the MNN. A. Trajectories of the MNN with various initial condition $(\mu(0), CV(0)) = (50, 1)$ and $(\mu(0), CV(0)) = (100, 1)$ (upper left, $\rho = 0$) $(\mu(0), CV(0)) = (50, .8)$ and $(\mu(0), CV(0)) = (100, 1)$ (upper right, $\rho = 0$), $(\mu(0), CV(0)) = (50, 1)$ and $(\mu(0), CV(0)) = (100, 1)$ (bottom left, $\rho = 0$), and $(\mu(0), CV(0)) = (50, 1)$ and $(\mu(0), CV(0)) = (100, 1)$ (bottom right, $\rho = 0.1$). Results are obtained with $r = 0, 0.1, 0.2, 0.3, 0.4, 0.5$. B. Input–output firing rate, typical sigmoidal function, although now the stable fixed points are $(\epsilon, 1)$ and $(\mu^*, 0)$.

Thus, owing to $\sigma = CV\sqrt{\mu}$, we obtain the derivative of f as follows:

$$\frac{\partial f}{\partial \mu} = \frac{[-p(1-r)\mu - V_{th}L]}{2\sqrt{(1+r^2)(p+(p-1)p\rho)}CV\mu^{3/2}} \exp\left(I_+^2\right)\int_{-\infty}^{I_+} \exp\left(-v^2\right)dv + \frac{(r-1)p + V_rL}{2\sqrt{(1+r^2)(p+(p-1)p\rho)}\mu CV} \exp\left(I_-^2\right)\int_{-\infty}^{I_-} \exp\left(-v^2\right)dv,$$

where

$$I_+ = \frac{V_{th}L - p(1-r)\mu}{\sqrt{(1+r^2)(p+(p-1)p\rho)}\sigma}, \quad I_- = \frac{V_rL - (1-r)\mu}{\sqrt{(1+r^2)(p+(p-1)p\rho)}\sigma},$$

according to $Vr = 0$ as we set.

We consider two situations: a small μ near zero and a large μ near infinity. On one hand, in the case of $\mu \to 0+$, we have

$$\frac{\partial f}{\partial \mu} \sim \frac{-V_{th}L}{2\sqrt{(1+r^2)(p+(p-1)p\rho)}CV\mu^{3/2}} \exp\left(I_+^2\right)\int_{-\infty}^{I_+} \exp\left(-v^2\right)dv$$

by neglecting the terms of higher orders. One can see that whether $r > 1$ or not, f is monotonically increasing with respect to small μ, which implies that the firing rate response increases with respect to the ascent of a small input firing rate.

Please cite this article as: Lu, W., et al., On a Gaussian neuronal field model, NeuroImage (2010), doi:10.1016/j.neuroimage.2010.02.075

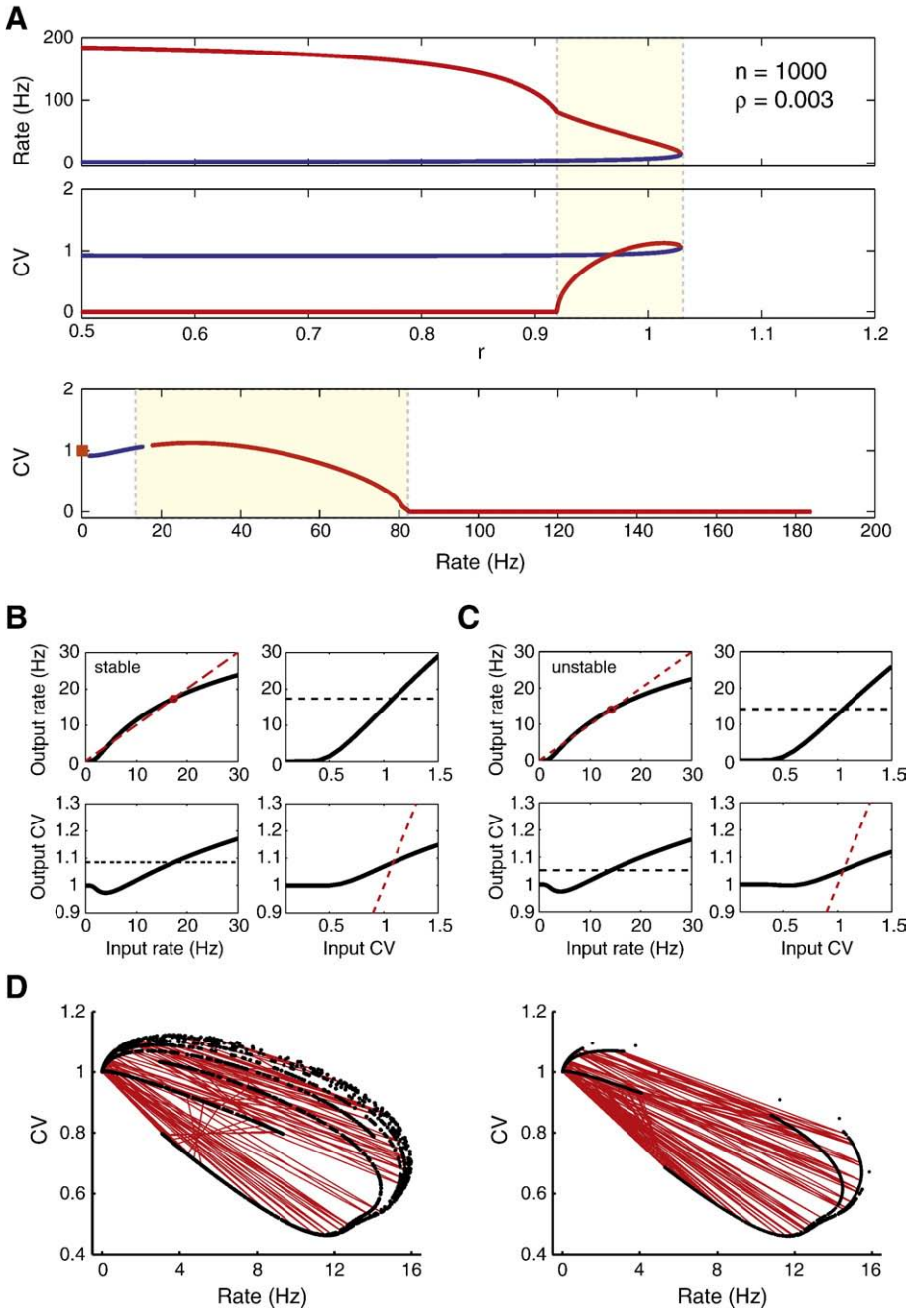

Fig. 3. The stable fixed points for $p=1000$, $\rho=0.003$. A. Output firing rate vs. r (upper trace), output CV vs. r (middle trace) and output CV vs. firing rate (bottom trace). The marked box corresponds the subthreshold input. B. Stable fixed point. C. Unstable fixed point. D. Neuronal activity with input. (For interpretation of the references to color in this figure legend, the reader is referred to the web version of this article.)

On the other hand, in the case of $\mu\to+\infty$, we have

$$\frac{\partial f}{\partial \mu}\sim\frac{[p(r-1)]}{2\sqrt{(1+r^2)(p+(p-1)p\rho)\mu CV}}\left[\exp\left(I_+^2\right)\int_{-\infty}^{I_+}\exp\left(-v^2\right)dv+\exp\left(I_-^2\right)\int_{-\infty}^{I-}\exp\left(-v^2\right)dv\right],$$

by neglecting the terms of lower orders. It is clear that if $r<1$, the firing rate response still increases according an ascent and large input firing rate; but if $r>1$, with a stronger inhibition than excitation, the situation turns over that the firing rate response decreases with respect the input firing rate of relative large values.

Therefore, as shown in the Fig. 1C, one can see that if $0<r<1$, the firing rate response function has the similar curve as the sigmoidal function. However, in the case of $r>1$, the plotting curve of the firing rate response function is near the shape of the tent or logistic map. And, the non-monotonicity and monotonicity shapes of the firing rate response function are distinguished as the critical value of the parameter r as:

$$r^*=1.$$

Please cite this article as: Lu, W., et al., On a Gaussian neuronal field model, NeuroImage (2010), doi:10.1016/j.neuroimage.2010.02.075

In the following, we illustrate the dynamical behaviour of the iterative Eq. (8) in the case of $r>1$. In Fig. 3, we plot the stable and unstable fixed points of the dynamics with a clamped correlation $\rho=0.003$. In additional to the trivial attractor $(0,1)$ (pseudo-silent state, filled red circle), we see that there is a gap between the pseudo-silence state and stable fixed firing rate. The lowest firing rate is around 15 Hz with a *CV* around 1 (red lines in Fig. 3A). When $r>1.03$, we see that the only stable fixed point is again the pseudo-silent state. The physical meaning is clear, when the inhibitory is strong enough, the network is silent. Figs. 3B and C tell us the reason why the fixed point disappears when $r>1.03$. This is simply because the firing rate is too low.

When $\rho=0.008$, a slightly increased correlation in comparison with Fig. 3, we see that now the stable fixed point is completely different as shown in Fig. 4. Note that there is always a fixed point solution for $r>0.5$ Fig. 4I A. The input–output firing rate is no longer a sigmoidal function and it starts to bend over Fig. 4I B. We point out here that for a model with exclusively firing rate such as the WCA model, it is impossible to have

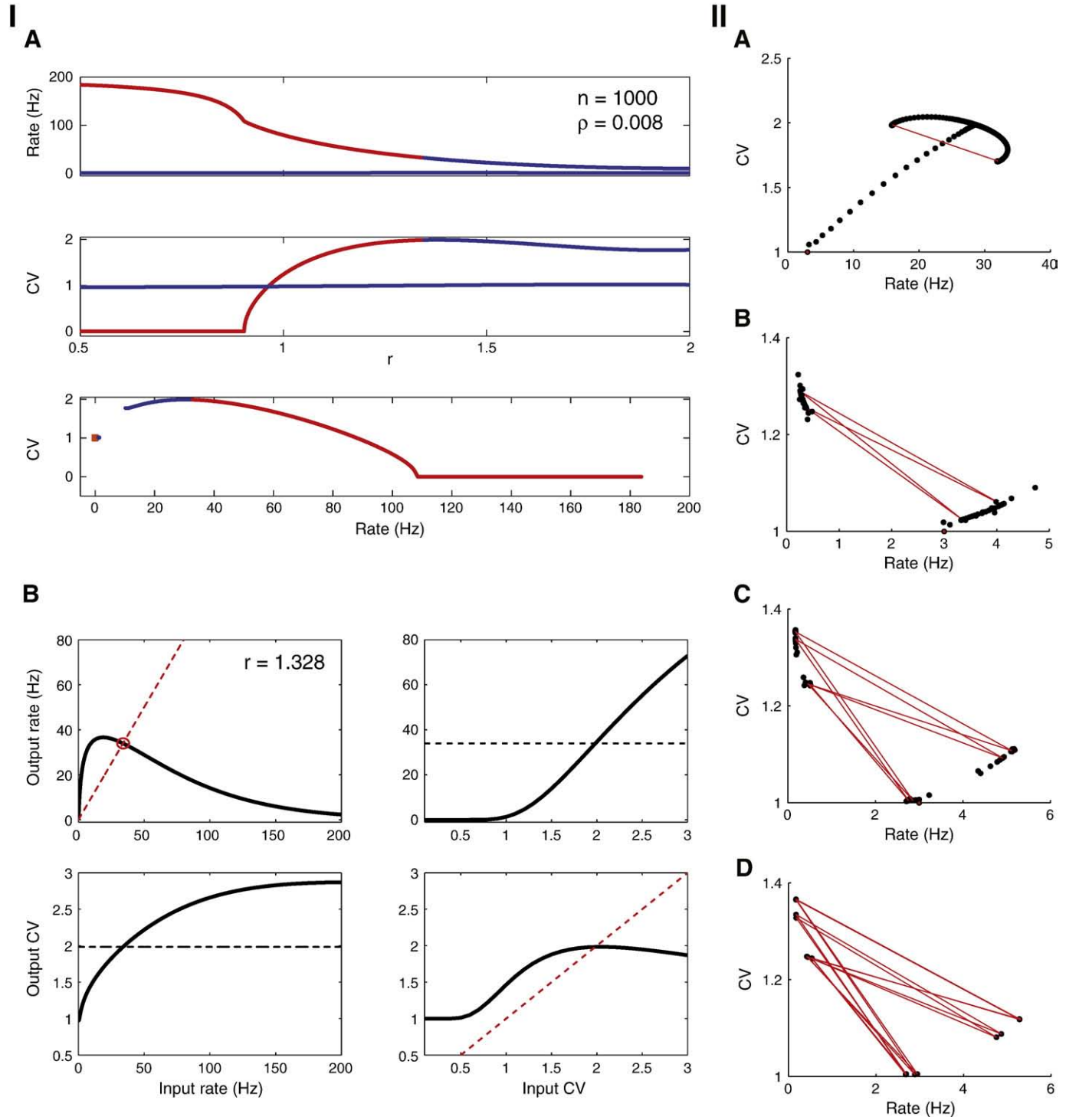

Fig. 4. Stable attractors for $p=1000$, $\rho=0.08$. A. Output firing rate vs. r (upper trace), output CV vs. r (middle trace) and output CV vs. firing rate (bottom trace). B. Detailed input–output relationship for the firing rate and CV for $r=1.328$. Note that it is not a sigmoidal function. C. From top to bottom, $r=1.4$ (period 2), $r=2.5$ (period 4), $r=2.8$ (period 8), and $r=3.8$ (period 16).

Please cite this article as: Lu, W., et al., On a Gaussian neuronal field model, NeuroImage (2010), doi:10.1016/j.neuroimage.2010.02.075

ARTICLE IN PRESS

such a non-monotonic input–output relationship. As shown in Figs. 4II A–D, with increasing $r>0$, the system has a periodic point with increasing periods. The firing rate map becomes bending like the tent or logistic map if the inhibition is strong. Since it is well-known that this shape of map in an iteration Eq. (8) may lead to complicated dynamical behaviours such as bifurcations even chaos, it is reasonable to expect the dynamics exhibits such rich behaviours. This will be one of our future research objectives to establish a clear spectrum of this neuronal field dynamics.

Synchronous spikes

We consider the map of coefficient of correlation:

$$\rho(x,y,k+1)=\chi(x,y,k)\frac{\langle \omega*\sigma,\omega*\sigma\rangle_{\rho(k)}(x,y)}{\|\omega*\sigma\|_{\rho(k)}(x)\|\omega*\sigma\|_{\rho(k)}(y)}. \tag{18}$$

It is a well-known fact in the literature that in a feedforward spiking neuronal network, spikes of different neurons could easily synchronize their activity (Reyes, 2003). This phenomenon has been an active topic in neuroscience research. It is clear that synchronization cannot be described by the WCA model, since the WCA model can only concern the first moment of the spiking activity but synchronization should be described by a second order statistics. Different from the literature (Diesmann et al., 1999; Mehring et al., 2003), the spike timing variation in pulse-packets is analyzed to study the synfire chain dynamics, in our Gaussian random field model, the correlation coefficients can serve to describe the synchronous motions in a neuronal field, i.e., we say that two neurons i and j (completely) *synchronize* if $\rho(i,j)=1$. Here, we try to prove this in a feedforward or recurrent spiking neuronal network with nonnegative interconnections, the correlation map could rapidly approach its stationary state under several setups.

We consider two setups for the topologies of the interactions between neurons:

1. Feedforward neuronal network: the topology is stochastically switching with respect to different iterations;
2. Recurrent neuronal network: the topology is static for all the time.

Using the results of the stability analysis of consensus algorithms (Olfati-Saber et al., 2007; Liu et al., 2009), we can derive the following results.

Theorem 3.3.1. *Suppose that $\chi(i,j,k)=1$, all couplings are nonnegative, and all variances are nonzero.*

1. *For a recurrent neuronal network, if the network has spanning trees,[2] then the neuronal network synchronizes with all coefficient of correlation equal 1;*
2. *For a feedforward neuronal network, if the expectation of the network has spanning trees, then the neuronal network synchronizes with all coefficient of correlation equal to 1 almost surely.*

See the mathematically formal depiction and proof in Appendix B.

Travelling waves

In some cases, the spiking activities can propagate over the field and grow to a static travelling wave of a fixed shape (Amari, 1977; Ermentrout and Kleinfeld, 2001; Nunez, 1974; Wu et al., 1999). The neuronal field model (WCA mode) can produce static travelling waves by simplifying the activations by the Heaviside function (Amari, 1977). Here, we use the similar idea to investigate the existence of a static travelling wave and its shapes in the Gaussian field. Since the response functions of the firing rate and variance are rather complicated and the number of equations is large, which makes difficult to study the evolution Eq. (9), we employ several simplifications. (1) We consider the Gaussian field in the continuous space of one dimension. (2) We clamp the correlation with a fixed value ρ. (3) The weight function $w(x,y)$ is picked as the Gaussian kernel function, i.e., $w(x,y)=\exp(-|x-y|^2/\gamma^2)$ for some $\gamma>0$. (4) We investigate the mean firing rate and variance of the neighborhood of the neuron instead of those of its own. Also, this section concerns the mathematics and the values of each variable do not have the same sense as in the sections above and afterwards. Let

$$\begin{aligned} u(x,t) &= \int w(x,y)\mu(p,t)dp,\\ v(x,t) &= \rho\int\int w(x,p)w(x,q)\sigma(p,t)\sigma(q,t)dpdq. \end{aligned}$$

Then Eq. (9) becomes:

$$\tau\dot{u}(x,t)=-u(x,t)+\int w(x,p)f(u(p,t),v(p,t))dp, \tag{19}$$

$$\tau\dot{v}(x,t)=-v(x,t)+\rho\left[\int w(x,p)g(u(p,t),v(p,t))dp\right]^2, \tag{20}$$

with the simplification $g(u,v)\approx u$ at the right-hand side. (5) We use the Heaviside function

$$H(z)=\begin{cases}1 & z>0\\ 0 & \text{otherwise}\end{cases}$$

[2] There exists one neuron which can access all other neurons by the couplings.

Please cite this article as: Lu, W., et al., On a Gaussian neuronal field model, NeuroImage (2010), doi:10.1016/j.neuroimage.2010.02.075

to approximate the firing rate response function with respect to the firing rate of the input spiking trains with small variances and so it is with the response function with respect to the variance of the input spike trains with small firing rates. Namely, we partly define

$$f(u,v) = \max\{H(u-u_0), H(v-v_0)H(u)\} \text{ and } g(u,v) = H(v-v_0)H(u).$$

According to Fig. 1C, these approximations are reasonable to certain degree.

We consider a neuronal field with two layers: one is an excitatory (E-) layer and the other is an inhibitory (I-) layer. The cells in the E-layer are interacted with both excitations and inhibitions described by the parameter r and send excitatory signal to the I-layers and the cells in the I-layer send inhibitory signals to the E-layers. We study the existence of the travelling waves under the situation that the variances in the I-layer are sufficiently small to be neglected. In details, we consider the following equations:

$$\begin{aligned}\tau\dot{u}^E(x) &= -u^E(x) + r_1\int w(x,p)f\left(u^E(p),v^E(p)\right)dp - r_2\int w(x,q)f\left(u^I(q),v^I(q)\right)dq + I,\\ \tau\dot{v}^E(x) &= -v^E(x) + \rho\left[\int w(x,p)g\left(u^E(p),v^E(p)\right)dp\right]^2,\end{aligned} \tag{21}$$

for the E-layer with some coefficient parameters $r_{1,2}$ and

$$\begin{aligned}\tau\dot{u}^I(x) &= -u^I(x) + w_0 f\left(u^E(x),v^E(x)\right) + J,\\ \tau\dot{v}^I(x) &= -v(x) + \varrho^2\left[g\left(u^E(x),v^E(x)\right)\right]^2.\end{aligned} \tag{22}$$

We consider the static travelling waves with the form $u^Y(x,t) = u^Y(x+ct)$ and $v^Y(x,t) = v^Y(x+ct)$ for some velocity c, $Y = I$ or E. Introducing a new variable $y = x+ct$, due to $\dot{u}^Y(x,t) = c\frac{du^Y}{dy}$ and $w(x,p) = w(x+ct, p+ct)$, Eqs. (21) and (22) become:

$$\begin{aligned}c\tau\frac{du^E}{dy} &= -u^E(y) + r_1\int w(x,p)f\left(u^E(p),v^E(p)\right)dp - r_2\int w(x,q)f\left(u^I(q),v^I(q)\right)dq + I,\\ c\tau\frac{dv^E}{dy} &= -v^E(y) + \rho\left[\int w(x,p)g\left(u^E(p),v^E(p)\right)dp\right]^2,\end{aligned} \tag{23}$$

and

$$\begin{aligned}c\tau\frac{du^I}{dy} &= -u^I(y) + w_0 f\left(u^E(y),v^E(y)\right) + J,\\ c\tau\frac{dv^I}{dy} &= -v(y) + \varrho^2\left[g\left(u^E(y),v^E(y)\right)\right]^2.\end{aligned} \tag{24}$$

In the following, we construct two examples of travelling wave solutions of these equations. In fact, we predesign the shapes of the waves and adjust the parameters to realize them. By these examples, we show that our model can have more elaborate shapes of travelling waves, compared with the first order model, for example WCA model (Amari, 1977).

Variance arousing bump of active firing rate

We construct a travelling wave of such a shape: the field of E-layer does not have an active firing rate, namely $u^E(y) < u_0$ for all y but has an active variance in the area $(0, a)$ for some $a > 0$, i.e., $v^E(y) > v_0$ if and only if $y \in (0, a)$. This static travelling wave at the E-layer arouse a narrow active interval (y_1, y_2) for some $y_{1,2}$, i.e., $u^I > u_0$ if and only if $y \in (y_1, y_2)$, and small variances $v^I(y) < v_0$. To obtain the values of the parameters to realize this shape of the travelling wave, we firstly consider the equation of v^E:

$$c\tau\frac{dv^E}{dy} = -v^E(y) + \rho\left[\int w(x,p)H\left(v^E(p)-v_0\right)dp\right]^2, \tag{25}$$

since we expect the $u^E(y) < u_0$ and $v^I(y) < v_0$ under the conditions mentioned below. Assuming $\lim_{y\to-\infty} v^E(y) = 0$, we can derive its solution as

$$v^E(y) = \frac{\rho}{\tau c}\int_{-\infty}^{y} \exp\left(\frac{y'-y}{\tau c}\right)\left[K\left(y'\right)\right]^2 dy'$$

with

$$K(y) = \int_0^a w\left(y,y'\right)dy' = \gamma\int_{-y}^{a-y}\exp\left(-u^2\right)du,$$

noting $w(y, y') = \exp(-(y-y')^2/\gamma^2)$. To ensure $v^E(y) > v_0$ only in $y \in (0, a)$, we give the following inequality:

$$v^E(y) > v_0 \forall y \in (0,a), \text{ and } v^E(0) = v^E(a) = v_0. \tag{26}$$

Please cite this article as: Lu, W., et al., On a Gaussian neuronal field model, NeuroImage (2010), doi:10.1016/j.neuroimage.2010.02.075

Second, we consider the equation of the $u^I(y)$. Due to the inactive firing rate at the E-layer, we have

$$c\tau\frac{du^I}{dy} = -u^I(y) + w_0 f\left(u^E(y), v^E(y)\right) + J$$

with some $J<0$ and a bump firing rate response function

$$f(u^E(y), v^E(y)) = \begin{cases} 1 & y\in(0,a) \\ 0 & otherwise. \end{cases}$$

Let $u^I(y)=J$ for all $y\le 0$. We get the solution of $u^I(y)$:

$$u^I(y) = \begin{cases} J & y\le 0 \\ w_0\left(1-\exp\left(-\frac{y}{c\tau}\right)\right)+J & 0<y<a \\ J + w_0\left(\exp\left(\frac{a}{c\tau}\right)-1\right)\exp\left(-\frac{y}{c\tau}\right) & y>a. \end{cases}$$

We expect to derive the active interval (y_1, y_2) of u^I by solving the following equations:

$$u^I(y_1) = u^I(y_2) = u_0. \tag{27}$$

Third, we consider the variance of the I-layer:

$$\tau c\frac{dv^I}{dy} = -v^I(y) + \varrho^2\left[g\left(u^E(y), v^E(y)\right)\right].$$

Due to $g(u^E(y), v^E(y))\le 1$ for all $y\in\mathbb{R}$, with assuming $v^I(y)=0$ for all $y<0$, it leads that the supremum value as

$$\sup_y v^I(y) = \varrho^2.$$

We expect that the variance $v^E(y)$ is too small to evoke variance at the E-layer, which demands

$$\varrho^2 < v_0. \tag{28}$$

Finally, we come back to the mean firing rate at the E-layer:

$$\begin{aligned} c\tau\frac{du^E}{dy} &= -u^E(y) + \int_{-\infty}^{\infty} w\left(y,y'\right)\left[r_1 f\left(u^E\left(y'\right), v^E\left(y'\right)\right) - r_2 f\left(u^I\left(y'\right), v^I\left(y'\right)\right)\right]dy' + I \\ &= -u^E(y) + \left[r_1\int_0^a w\left(y,y'\right)dy' - r_2\int_{y_1}^{y_2} w\left(y,y'\right)dy'\right] + I, \end{aligned}$$

owing to the expected results for this system as mentioned above. Let

$$K_1(y) = \int_0^a \exp\left(-\frac{\left(y-y'\right)^2}{\gamma^2}\right)dy', K_2(y) = \int_{y_1}^{y_2}\exp\left(-\frac{\left(y-y'\right)^2}{\gamma^2}\right)dy'.$$

Assuming $u^E(-\infty)=0$, we can have the solution in the form:

$$u(y) = \int_{-\infty}^{y}\exp\left(\frac{y-y'}{c\tau}\right)\frac{1}{c\tau}\left[r_1 K_1\left(y'\right) - r_2 K_2\left(y'\right) + I\right]dy'.$$

To ensure $u^E(y)>0$ only on $y\in(0, a)$ and $u^E(y)<u_0$ for all y as we expect, we need

$$u^E(0) = u^E(a) = 0. \tag{29}$$

In summary, if we can solve the Eqs. (26) and (27) and inequations (28) and (29) to derive positive solutions for c and a, as well as some $y_2>y_1$, the static travelling wave, as we designed, exists for the simplified Gaussian field equation of the MNNs. Numerical methods can be utilized for illustration. We pick $c=3.1064$, $\tau=10$, $\gamma=5$, $v_0=u_0=0.1$, $\rho=0.1$, $r_1=0.1$, $r_2=0.5378$, $I=0.0368$, $J=-0.3152$, $w_0=1.6089$, we have the solutions of travelling waves with $a=10$, $y_1=9.2730$, and $y_2=12$. As shown in the left plot of Fig. 5A, the firing rate of the E-layer is not strong enough to evoke spikes at the I-layer but the variance at $(0, a)$ is large enough. This still evoke a bump of firing rate at the I-layer as shown in the left plot of Fig. 5C.

Two bumps of firing rate and variance respectively arousing bump of firing rate with two peaks

We construct a static travelling wave solution of the other shape: the E-layer has a bump of firing rate and a bump of variance in different spatial interval, (a, b) and $(0, d)$ with $d>0>b>a$, respectively, which evoke one bump of activity of firing rate at the I-layer with two peaks with $u^I(y)>u_0$ at the spatial intervals (y_1, y_2) and (y_3, y_4) but the variances at I-layer are all smaller than v_0.

Please cite this article as: Lu, W., et al., On a Gaussian neuronal field model, NeuroImage (2010), doi:10.1016/j.neuroimage.2010.02.075

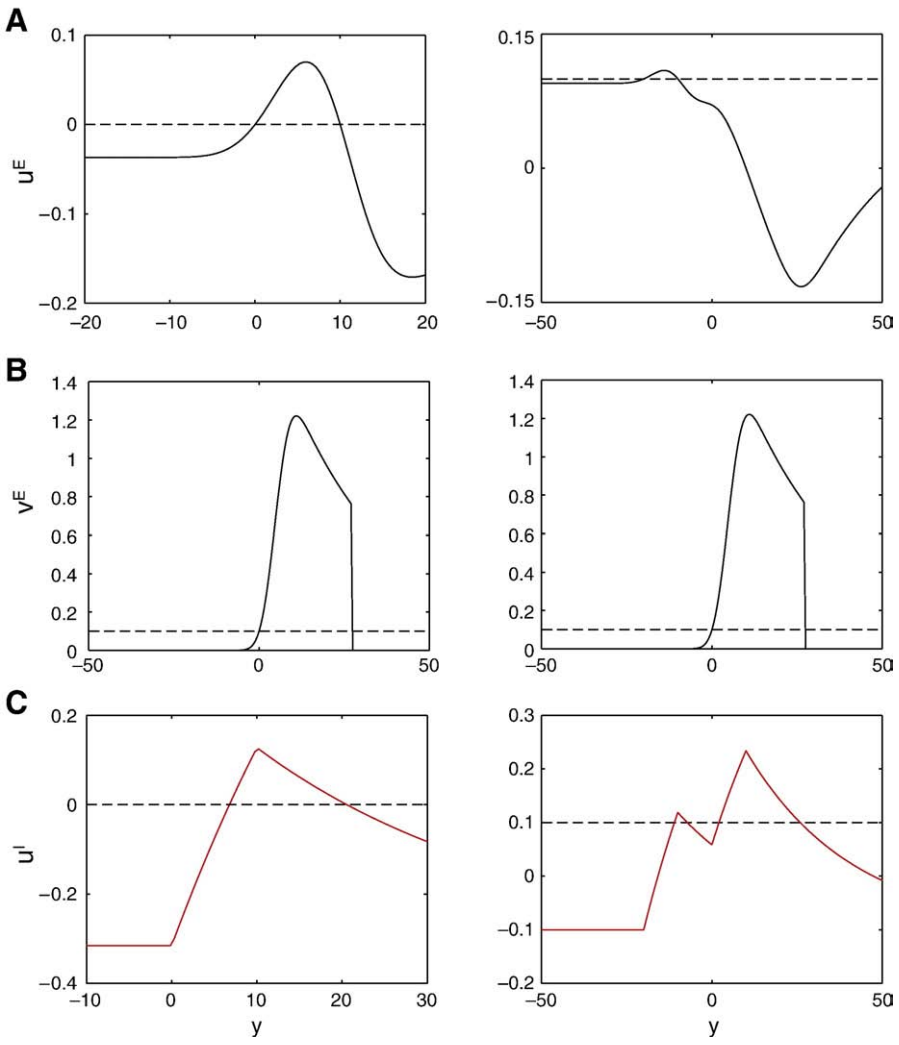

Fig. 5. The traveling wave solutions of the firing rate and variance at the *E*-layer: The bumps of the traveling wave solution of the firing rate at the *I*-layer. The left plots in A–C for the first example: variance arousing bump of active firing rate, are the traveling waves with respect to the firing rate and variance at the *E*-layer, and the firing rate at the *I*-layer, respectively. The right plots of A–C for the second example: two bumps of firing rate and variance respectively arousing bump of firing rate with two peaks, are the traveling waves with respect to the firing rate and variance at the *E*-layer, and the firing rate at the *I*-layer, respectively.

First, we consider that the $v^E(y)$ is larger than v_0 if and only if $y \in (0, d)$ and expect that the variance at the *I*-layer is too small to be taken into considerations to the *E*-layer. So, with the same algebras, we can get the equation as the similar form as Eq. (26):

$$v^E(d) = v^E(0) = v_0, \text{ and } v^E(y) > v_0, \forall y \in (0, d). \tag{30}$$

Second, we expect that $u^E(y) > u_0$ at $y \in (a, b)$ and $u_0 > u^E(y) > 0$ in $y \in (0, d)$ with $u^E(d) = 0$. Combined with $v^E(y) > v_0$ at $y \in (0, d)$ with $v^E(0) = v_0$, we have the equation of $u^I(y)$ as

$$c\tau \frac{du^I}{dy} = -u^I(y) + \omega h(y) + J,$$

$$h(y) = \begin{cases} 1 & y \in (a, b) \cup (0, d) \\ 0 & otherwise. \end{cases}$$

Letting $u^I(y) = J$ for all $y \le a$, we have

$$u^I(y) = \begin{cases} J & y < a \\ J + w_0\left(1 - \exp\left(\frac{a-y}{c\tau}\right)\right) & a \le y < b \\ J + w_0\left(\exp\left(\frac{b}{c\tau}\right) - \exp\left(\frac{a}{c\tau}\right)\right)\exp\left(\frac{-y}{c\tau}\right) & b \le y < 0 \\ J + w_0\left(\exp\left(\frac{b}{c\tau}\right) - \exp\left(\frac{a}{c\tau}\right)\right)\exp\left(\frac{-y}{c\tau}\right) + w_0\left(1 - \exp\left(\frac{-y}{c\tau}\right)\right) & 0 \le y < d \\ J + w_0\left(\exp\left(\frac{b}{c\tau}\right) - \exp\left(\frac{a}{c\tau}\right)\right)\exp\left(\frac{-y}{c\tau}\right) + w_0\left(\exp\left(\frac{d}{c\tau}\right) - 1\right)\exp\left(\frac{-y}{c\tau}\right) & y > d. \end{cases}$$

Please cite this article as: Lu, W., et al., On a Gaussian neuronal field model, NeuroImage (2010), doi:10.1016/j.neuroimage.2010.02.075

To guaranteeing evoking a bump of positive active rate with two peaks: $u^I(y)>u_0$ in the interval (y_1, y_2) and (y_3, y_4) with $y_4>y_3>y_2>y_1$, as we designed, we need

$$u^I(y_1) = u^I(y_2) = u^I(y_3) = u^I(y_4) = u_0. \tag{31}$$

Third, similarly with Ineq. (28) we need $v^I(y)<v_0$ for all $y\in R$, which implies that the following

$$\varrho^2<v_0 \tag{32}$$

is necessary.

Finally, we consider the equation with respect to $u^E(y)$ without external inputs:

$$c\tau\frac{du^E}{dy} = -u^E(y) + r_1\left[\int_a^b w(y,y')dy' + r_1\int_0^d w(y,y')dy'\right] - r_2\left[\int_{y_1}^{y_2} w(y,y')dy' + \int_{y_3}^{y_4} w(y,y')dy'\right] + I.$$

So, letting $u^E(-\infty)=0$, we have the solution:

$$u^E(y) = \frac{1}{c\tau}\int_{-\infty}^{y}\exp\left(\frac{y'-y}{c\tau}\right)\{r_1[W_1(y') + W_2(y')] - r_2[W_3(y') + W_4(y')] + I\}dy',$$

with

$$W_1(y) = \int_a^b \exp\left(-\frac{(y-y')^2}{\gamma^2}\right)dy', W_2(y) = \int_0^d \exp\left(-\frac{(y-y')^2}{\gamma^2}\right)dy',$$

$$W_3(y) = \int_{y_1}^{y_2}\exp\left(-\frac{(y-y')^2}{\gamma^2}\right)dy', W_4(y) = \int_{y_3}^{y_4} exp\left(-\frac{(y-y')^2}{\gamma^2}\right)dy'$$

To guarantee $u^E(y)>u_0$ only at $y\in(a, b)$, $u_0>u^E(y)>0$ at $(0, d)$, and $u^E(y)<0$ for all $y>d$ and $y<a$, we need

$$u^E(a) = u^E(b) = 0, \quad u^E(d) = 0. \tag{33}$$

In summary, if we can get positive d and c as well as $y_2>y_1$ and $d>a$ from Eqs. and Ineq. (30)–(33), then we can generate a static travelling wave solution with the shape we predesigned. In numerical illustrations, we pick $c=3.1064$, $\tau=10$, $\gamma=5$, $\rho=0.1$, $u_0=v_0=0.1$, $I=0.0214$, $r_1=0.0134$, $r_2=0.0548$, $J=-0.1$, $w_0=0.7951$, we can have solutions of travelling waves with $a=-20$, $b=-10$, $d=10$, $y_1=-11$, $y_2=-7.2016$, $y_3=2.0883$, and $y_4=25.9131$. As shown in the right plots of Fig. 5A, (a, b) are the only interval at E-layer such that the firing rate is enough to evoke spikes at the I-layer. However, combined with the variance at the E-layer as shown in the right plot of Fig. 5B, there is a bump of firing rate at the I-layer with two peaks (two intervals with firing rate larger than u_0), as indicated in the right plot of Fig. 5C.

Working memory: neuronal computation with MNNs

Towards a working memory task, we consider a population of N neurons with connection weights given by

$$w_{ij} = c\sum_{p=1}^{P}\left(\xi_i^p - \overline{\xi}_i\right)\xi_j,$$

where c is a constant and $\{\xi^p\}_{p=1,\cdots,P}$ are the stored patterns, with $\xi_i^p\in\{0, 1\}$, $i=1, \cdots, N$, $p=1, \cdots, P$, and

$$\overline{\xi}_i = \frac{1}{P}\sum_{p=1}^{P}\xi_i^p.$$

Each neuron is subject to an external stimulus given by

$$\overline{\mu}_{\mathrm{ext},i}(t) = \overline{\mu}_{b,i}(t) + \mu_{s,i}(t),$$

where the first term represents a noisy background and the second a stimulus-dependent input. In particular, we define the background input as $\overline{\mu}_{b,i}(t)=\overline{\mu}_b\zeta_i(t)$, where $\zeta_i(t)\in\{0, 1\}$ are i.i.d. Bernoulli random variables with $P(\zeta_i(t)=1)=p_b$. That is, at each iteration, a subset of neurons, chosen randomly and independently on the pattern to retrieve, is subject to an input of fixed size. The stimulus-dependent input is defined by $\overline{\mu}_{s,i}(t)=\overline{\mu}_s h_i\theta(t-t_1)\theta(t_2-t)$, where $h_i=(\xi_i^1+n_i)$ mod 2, and n_i are i.i.d. Bernoulli random variables with $P(n_i=1)=p_n$. That is, a stimulus partly correlated with one of the patterns is applied continuously during a finite (short) interval of time. Finally we assume the external input is Poisson, therefore we set

$$\overline{\sigma}_{\mathrm{ext},i} = \overline{\mu}_{\mathrm{ext},i}(t).$$

Please cite this article as: Lu, W., et al., On a Gaussian neuronal field model, NeuroImage (2010), doi:10.1016/j.neuroimage.2010.02.075

ARTICLE IN PRESS

For our simulations, we considered a system of $N=2500$ neurons and a set of 8 patterns, which are illustrated in Fig. 6A. The values of the other parameters were set as follows: $c=0.9375$, $p_n=0.2$, $\overline{\mu}_b=0.6\mu_{th}$, $p_b=0.2$, $\overline{\mu}_s=\mu_{ths}$, $t_1=3$, $t_2=5$. We assumed all the neurons are silent on Iteration 0.

The plots in Fig. 6B show the firing rate, the CV of the output inter-spike intervals, the mean and variance of the total input (recurrent plus external) to each neuron, recorded at different iterations. The last two plots in Fig. 6B show the pairwise correlation between one cell belonging (resp. not belonging) to pattern to be recalled and all the other cells in the network. Fig. 6C shows the overlaps between the vector of firing rates and each one of the patterns, $o^p(t)=\langle \nu(t), \xi^p \rangle$, over successive iterations.

To fully explore the advantages of our MNN approach on working memories is out of the scope of the current paper. Different from the results reported by Brunel and Wang (2001), Deco and Rolls (2003), here our stimuli are content-dependent, but in their papers, all stimuli are simply a constant firing rate.

Conclusions, prospects and discussions

When modelling neuronal networks, it is important to construct mathematical models to describe the neuronal networks via biological knowledge and theories. For example, the well-known leaky integrate-and-fire and Hodgkin–Huxley models, described via differential equations, can precisely describe the configuration and function of a single neuron. However, when coupling a large number of such differential equations to model neuronal networks, it is a difficult to analyze the dynamical behaviour of spike trains by a mathematically clear and rigorous manner. Most of the work is done via numerical approaches. Despite being able to dig much knowledge, it is still difficult to employ statistical methods to directly handle real-world experimental data via these models in a rigorous mathematical manner. On the other hand, the well-developed statistical methods have been widely used in neural signal processing. One of the most useful methods is random field, including Gaussian random field (GRF), Markov random field (MRF), conditional random field (CRF), and it provides powerful and robust treatments to data from experiments, for instance, LFP, fMRI, and EEG/MEG, concerning their coding/decoding functions. However, despite being conveniently realizable in mathematics, the model describing the neuronal system is rather simple and is regarded as a linear signal transformer (Firston et al., 1995), or sometimes as simply nonlinear, with high dimensions. In these models, the neuronal system is regarded as a signal transformer and has no difference from man-made signal systems.

A possible trade-off to handle this paradox is to model neuronal networks via some well-defined single neuron model with certain simplifications and approximations that allows well-developed statistical methods to be employed to associate model activities with experimental data. In this paper, continuing from the previous work (Feng et al., 2007), we use coupled LIF neurons with the renewal theory, the OU process theory, and some simplifications. In details, we treat neuronal spikes as renewal processes, only considering the first and second statistics, and regard them as time-varying stationary processes, to build a Gaussian random field to describe the temporal and spatial distribution of spike trains in the neuronal network.

We expect, in future work, under the MNN framework, that the classic statistical approaches, for example, the Bayesian approach, can be employed. Furthermore, this idea can be extended to generalized LIF neuron models, for example, the nonlinear LIF neuron. If necessary, we can include other higher order statistics to describe the PDF. See Appendix C for an example and it will be one of the foci of our future research. Furthermore, we also expect that the methodology of Gaussian random field can be applied to describe other biological data in additional to neuronal spikes, for instances, LFP, fMRI, and EEG/MEG. How to employ this methodology to deal with LFP, fMRI, and EEG/MEG data will also be the focus of our future research.

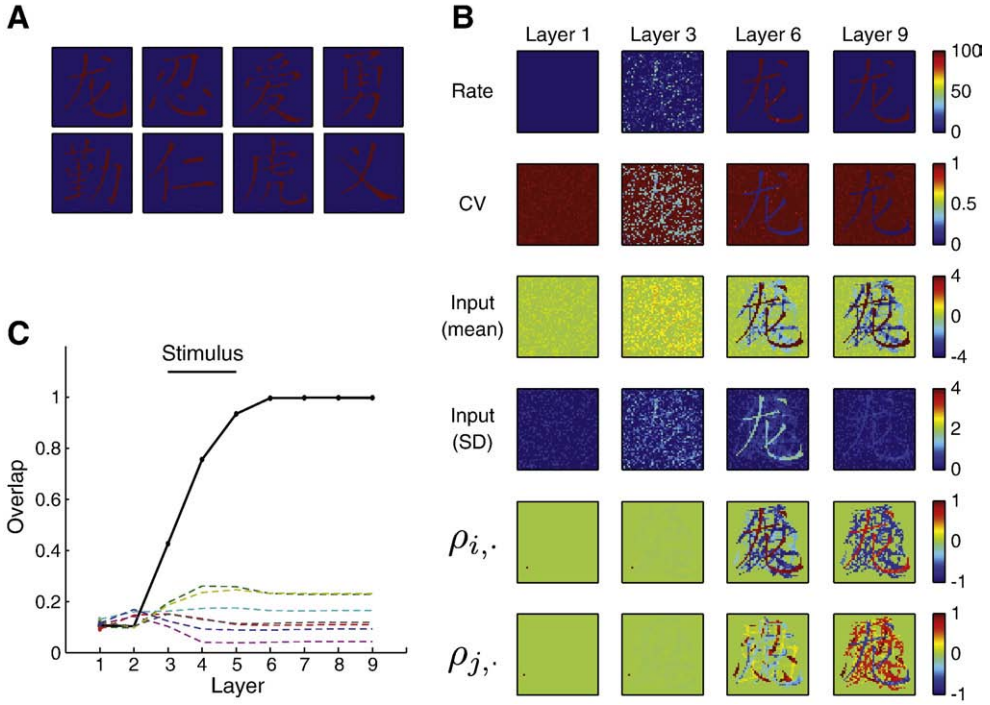

Fig. 6. Working memory in MNN. A. Eight Chinese characters are stored in the networks. B. Activities of rate, CV, input mean, input CV and correlations are plotted for iteration 1, iteration 3, iteration 6 and iteration 9. C. Overlaps of the retrieved memories after a brief stimulation.

Please cite this article as: Lu, W., et al., On a Gaussian neuronal field model, NeuroImage (2010), doi:10.1016/j.neuroimage.2010.02.075

Random field of LFP

A local field potential (LFP) is a class of electrophysiological signals and is believed to be the sum of all dendritic synaptic activity within a volume of tissue. LFPs can be regarded as the input into the observed area, opposite to neuronal spikes which represent the output of neurons. When measuring LFPs in an area, both temporal and spatial distributions are key to our study. In Fig. 7 we compute the distribution of the first order (mean) and the second order statistics (standard variance and the coefficients of correlation) of LFPs. The data comes from sheep IT (see Kendrick et al. (2009) for experimental details) with respect to the time, via 64 electrodes recordings. As Figs. 7A and B show, the mean and the variance both show clear spatial distribution patterns with similarity. Also, as shown in the snapshots (Figs. 7C–F), the coefficients of correlation exhibit rich content. There are two clusters, in which the neurons are almost synchronized, and the inter-correlations between the clusters have diversity, including synchronization, de-synchronization and non-correlations. Therefore, when constructing a stochastic model to describe LFPs, one should take time and space into considerations: it is truly a random field.

Random field of fMRI, EEG/ MEG

Functional magnetic resonance imaging (fMRI), electroencephalograph (EEG) and magnetoencephalograph (MEG) are popular techniques that study brain functions under various cognitive and behavioural tasks. In model-based methods, a statistical parametric map of brain activation is built by examining the time-series response of each voxel in the brain. For instance, in mathematical terms, the processing of fMRI constructs a map from the image space of fMRI to the pattern space of the behaviours. In the recent literature, the fMRI is regarded as a natural image and modelled as random fields. For instance, they use a GRF to describe the basic properties of the image (Friston et al., 1994), use a MRF to provide the interactions between subregions (Svensén et al., 2000), use a CRF to state the map from the activation region labels to the observed data (Wang and Rajapakse, 2006), or a non-central RF to calculate the power (Hayasaka et al., 2007). Then, they use the imaging data as samples which are supposed to be statistically independent within the observed time bins. And, the parametric map is constructed from the behaviours to the activation data. These methods are also employed to deal with EEG/MEG data (Caronell et al., 2009; Pantazis et al., 2005). Despite its success in the past few years, the model is simple and linear and the relations between physiological configurations and the activation map are unclear. Moreover, the time varying within the observed time bin is always neglected, which makes it difficult to describe the short-term dynamical properties such as the short-term memory. Therefore, it would be better to model the objective data from fMRI and EEG/MEG as a random field with respect to both space and time.

Computation with second order statistics

The firing rate is the popular variable in experiments or in modelling (Deco et al., 2008). The famous WCA model was proposed as a field model to describe neuronal dynamics. However, there are many situations, where the first order statistics are far from sufficient in describing neuronal activity. These phenomena include emergent collective behaviours, for instance, the correlated neuronal activities (Feng and Brown, 1999; Feng and Brown, 2000; Romo et al., 2004; De La Rocha et al., 2007), which are clearly related to the second order statistics (the coefficients of correlations and the CVs). Moreover, to

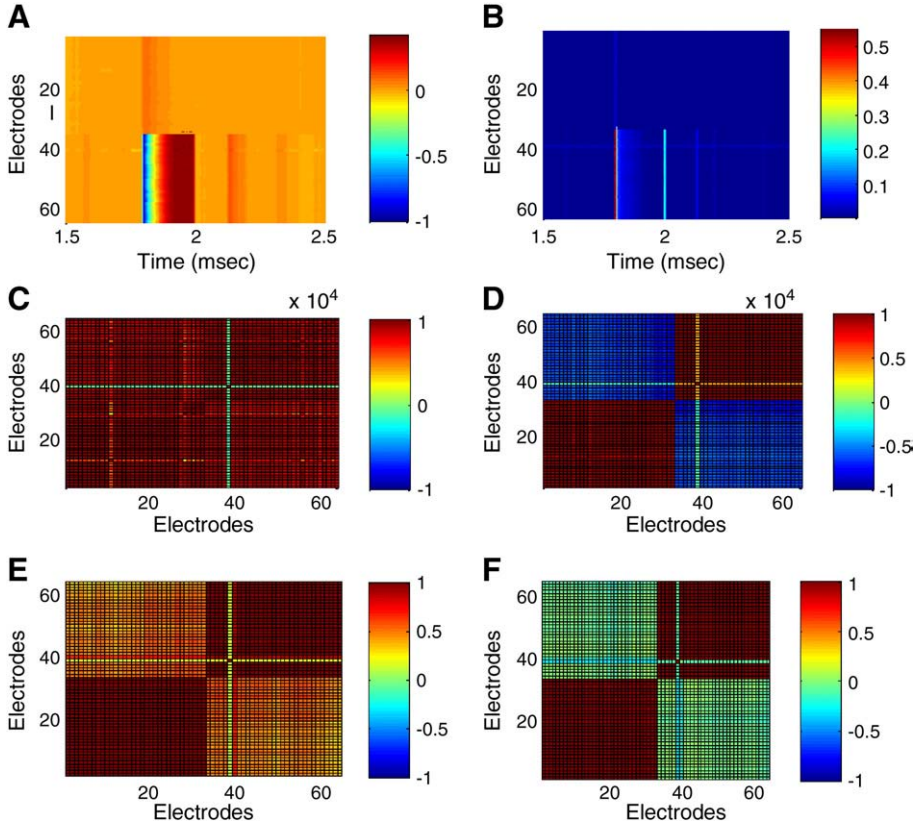

Fig. 7. The distributions of the mean, variance, and coefficients of correlations of LFPs of 64 electrodes from the data provided by Kendrick et al. (2009) with respect to both space (electrodes) and time. A. The distribution of the mean: The mean at the time t is computed over a time bin with 100 ms and centered at t. The unit of the potential is mV; B. The distribution of the variances of the LFPs of 64 electrodes: The variance at the time t is computed over a time bin with 100 ms and centered at t. The unit of the potential is mV; C–F. the snapshots of the spatial distributions of the coefficients of correlations at different time: $t=17$ s (C), $t=19$ s (D), $t=23$ s (E), and $t=25$ s (F).

Please cite this article as: Lu, W., et al., On a Gaussian neuronal field model, NeuroImage (2010), doi:10.1016/j.neuroimage.2010.02.075

ARTICLE IN PRESS

employ the Bayesian or any stochastic approach to analyze neuronal spikes, we have to consider the second order statistics. In the previous section, we have carried out a study on working memories. As the example demonstrates, the second order statistics including the CV of ISIs and their correlations have the capability to perform the working memory task. In particular, the CVs can clearly recall the input at an earlier iteration than the firing rate. More tasks will be investigated to assess the difference and relationship between the signal processing capabilities of the first and the second order statistics in our future research.

Limitations of our model

As all models in neuroscience, it is clear that our model has several limitations. First, we use the renewal approximation, i.e. we the use renewal point process to approximate the spike dynamics. By this approximation, the temporal-correlations in one spike train are indeed neglected. Second, we only consider finite order moments, essentially two here. Despite gaining more suitable information to describe experimental data than the first order model, it is still limited since higher order moments might contain information. Third, in the continuous-time model, we consider the stationary distribution at each time, which implies that we use a relatively slow time scale to derive the differential equations, similar to the derivation of the WCA model. To further explore the influence of these limitations is one of our future research objectives. In addition, the LIF neuron model used here does not contain the contents of the synaptic response, which has more realistic biological meaning. We think that using a similar approach, we can extend our analysis here to a more biologically realistic case. For example, the synaptic input composes of AMPA, NMDA, $GABA_A$ and $GABA_B$, which will be one of our future research topics.

Acknowledgments

W. L. Lu is supported by the National Natural Sciences Foundation of China under grant no. 60804044, and the Shanghai Pujiang Program no. 08PJ14019, and J. F. Feng is supported by an EPSRC (UK) grant CARMEN. We also acknowledge the financial support of the Future and Emerging Technologies (FET) programme within the Seventh Framework Programme for Research of the European Commission, under the FET-OPEN grant agreement BION, number 213219.

Appendix A. Correlation maps

In this appendix, we try to derive the map of the coefficients of correlations. The main approach of this part comes from the linear perturbation theory as shown in (De la Rocha et al., 2007; Gammaitoni et al., 1998) with minor modifications. Since we approximate the input spike trains by Gaussian motions, it is equivalent to study the correlation between two OU processes with correlated Brownian motion inputs. First, we consider the coefficient of the correlation. Consider two correlated OU processes:

$$\begin{cases} dV_1 = -LV_1dt + \hat{\mu}_1 dt + \hat{\sigma}_1 dW_1, \\ dV_2 = -LV_2dt + \hat{\mu}_2 dt + \hat{\sigma}_2 dW_2 \end{cases},$$

where dW_1 and dW_2 are two correlated Winier processes with correlation ρ_{in}. Thus, we can rewrite them as

$$\begin{cases} dW_1 = \sqrt{1-|\rho_{in}|}dW_a + \sqrt{|\rho_{in}|}dW_c \\ dW_1 = \sqrt{1-|\rho_{in}|}dW_b + \sqrt{|\rho_{in}|}dW_c \end{cases},$$

where $dW_{a,b,c}$ are independent Winier processes. Let $y_i(t)$ be the spike train subtracting the mean of the i-th neuron, $\tilde{y}_i(\omega)$ be its Fourier transformation, and $\tilde{C}_{ij}(\omega) = \lim_{T\to\infty}\langle \tilde{y}_i^* \tilde{y}_j \rangle$, which is the Fourier transformation of the correlation. We consider the situation near $\rho_{in} = 0$. Omitting the terms higher than 1, we have

$$\tilde{y}_i(\omega) \sim \tilde{y}_{i,0}(\omega) + A_i(\omega)\tilde{Q}_i(\omega), \quad i = 1, 2, \text{ as } \omega \to 0, \tag{34}$$

where $\tilde{y}_{i,0}(\omega)$ is the Fourier transformation of the spike trains of the neuron i in case of $\rho_{in} = 0$ and $\tilde{Q}(\omega)$ is the Fourier transformation of the Winier process $\pm\sigma_i\sqrt{|\rho_{in}|}dW_c/dt$ according to the input. So, we have

$$\begin{aligned} \tilde{C}_{ij}(\omega) \simeq & \langle \tilde{y}_{i,0}^* \tilde{y}_{j,0} \rangle + \langle A_j \tilde{Q}_j \tilde{y}_{i,0}^* \rangle + \langle A_i^* \tilde{Q}_i^* \tilde{y}_{j,0} \rangle + A_i^* A_j \langle \tilde{Q}_i^* \tilde{Q}_j \rangle \\ & = A_i^* A_j \langle \tilde{Q}_i^* \tilde{Q}_j \rangle, \end{aligned}$$

since $y_{i,0}$ and Q_i, $i = 1, 2$, are independent and the pair of $y_{i,0}$ and $y_{j,0}$ and the pair of Q_i and Q_j are independent respectively. From De La Rocha et al. (2007), noting

$$\int_{-\infty}^{\infty} d\tau C_{ij}(\tau) = \int_{-\infty}^{\infty} d\tau \exp(-i0\tau) C_{ij}(\tau) = \tilde{C}ij(0) \simeq A_i^* A_j \tilde{C}_{Q_i,Q_j}(0)$$

and

$$\lim_{\omega\to 0} A_i(\omega) = \frac{d\mu_i}{d\hat{\mu}_i}, \int_{-\infty}^{\infty} C_{ii}(\tau)d\tau = \mu_i CV_i^2, \tilde{C}_{Q_i,Q_j}(0) = \hat{\sigma}_i\hat{\sigma}_j\rho_{in},$$

we can formulate the output correlation as follows

$$\rho_{out} = \frac{\int_{-\infty}^{\infty} d\tau C_{ij}(\tau)}{\sqrt{\int_{-\infty}^{\infty} d\tau C_{ii}(\tau)}\sqrt{\int_{-\infty}^{\infty} d\tau C_{jj}(\tau)}} = \frac{\hat{\sigma}_i\hat{\sigma}_j \frac{d\mu_i}{d\hat{\mu}i}\frac{d\mu_j}{d\hat{\mu}j}}{CV_i CV_j\sqrt{\mu_i\mu_j}}\rho_{in}. \tag{35}$$

Here, the variables in the formula above are expressed as follows:

$$\mu_i = \left(T_{ref} + \frac{2}{L}\int_{I(V_r,\hat{\mu}_i,\hat{\sigma}_i)}^{I(V_{th},\hat{\mu}_i,\hat{\sigma}_i)} D_-(u)du\right)^{-1} = S_1(\hat{\mu},\hat{\sigma}),$$

$$CV_i = \sqrt{\mathrm{var}(T_i)}\mu_i = \frac{\left(\frac{8}{L^2}\int_{I(V_r,\hat{\mu}_i,\hat{\sigma}_i)}^{I(V_{th},\hat{\sigma}_i,\hat{\sigma}_i)} D_- \otimes D_+(u)du\right)^{1/2}}{T_{ref} + \frac{2}{L}\int_{I(V_r,\hat{\mu}_i,\hat{\sigma}_i)}^{I(V_{th},\hat{\mu},\hat{\sigma})} D_-(u)du} = S_2(\hat{\mu},\hat{\sigma}),$$

$$\begin{aligned} \frac{d\mu_i}{d\hat{\mu}_i} = & \frac{2\mu_i^2}{L^{3/2}\hat{\sigma}_i}\Big[\exp\left((I(V_{th},\hat{\mu}_i,\hat{\sigma}_i))^2\right)\int_{-\infty}^{I(V_{th},\hat{\mu}_i,\hat{\sigma}_i)}\exp\left(-v^2\right)dv \\ & - \exp\left((I(V_r,\hat{\mu}_i,\hat{\sigma}_i))^2\right)\int_{-\infty}^{I(V_r,\hat{\mu}_i,\hat{\sigma}_i)}\exp\left(-v^2\right)dv\Big], i = 1, 2. \end{aligned}$$

Appendix B. Proof of theorem 1

First, we give the mathematically formal depiction of Theorem 3.3.1. We consider the discrete space distribution of the neuron locations. Let $i = 1, \cdots, p$ be the index for a neuron and $W(k) = [W(i, j, k)]_{i,j=1}^{p}$ be the interconnection weight matrix, where $W(i, j, k)$ is the weight from the j-th neuron to the i-th neuron at the k-th iteration or the time k. Here, we assume all interconnections nonnegative, namely, $W(i, j, k) \geq 0$.

We can denote the graph corresponding to a nonnegative matrix $A = [A(i, j)]_{i,j=1}^{N}$, where N is the number of nodes by the way that $A(i, j) > 0$ if and only if there exists a link from neuron j to i. We denote by $\mathcal{G}(A)$ the graph corresponding to the nonnegative matrix $A = [A(i, j)]_{i,j=1}^{N}$. If A varies with respect to time, i.e., A^k, $k = 1, 2, \cdots$, then we can accordingly denote a series of graphs $\mathcal{G}(A^k)$ by the same manner mentioned above. In this situation, we define a δ-graph of $\mathcal{G}(A)$ for some $\delta > 0$ by the manner that there exists an link from j to i if and only if $A(i, j) > \delta$.

Theorem 4.4.1. *Suppose that*

1. *$\chi(i, j, k) = 1$ for all i, j and k;*

Please cite this article as: Lu, W., et al., On a Gaussian neuronal field model, NeuroImage (2010), doi:10.1016/j.neuroimage.2010.02.075

ARTICLE IN PRESS

2. *all matrices $W(k)$ are nonnegative matrices and have bounded elements and there exists $e>0$ such that the self-links are positive and $W(i,i,k)>e$ for all $i=1,\cdots,p$ and $k=1,2,\cdots$;*
3. *there exists some $\sigma_0>0$ such that $\sigma(i,k)\geq\sigma_0$ for all i and k.*

Then, we have

1. *For a recurrent neuronal network, if the corresponding graph $\mathcal{G}(W)$ has spanning trees, then for any nonnegative initial values, $\lim_{k\to\infty}\rho(i,j,k)=1$ holds for all $i\neq j$.*
2. *For a feedforward neuronal network, additionally supposing that each element $W(k)$ is an adaptive stochastic process associated with the σ-algebras $\mathcal{F}_k$,[3] if there exist some $K\in N$ and $\delta>0$ such that the δ-graph corresponding to the conditional expectation*

$$E\left[\sum_{k=lK+1}^{(l+1)K} W(k)\,|\,\mathcal{F}_{lK}\right]$$

has spanning tree almost surely for all l, then for any nonnegative initial values and almost every sequence of $\{W(k)\}_{k=1}^{\infty}$, $\lim_{k\to\infty}\rho(i,j,k)=1$ holds for all $i\neq j$.

Proof. Let $\rho(k)=[\rho(i,j,k)]_{i,j=1}^{p}$ and $V(i,j,k)=W(i,j,k)\sigma(j,k)$ with $V(k)=[V(i,j,k)]_{i,j=1}^{p}$. We rewrite the evolution of the correlations as

$$\begin{aligned} B(k) &= V(k)\rho(k)V^{\top}(k)\\ \rho(i,j)(k+1) &= \frac{B(i,j,k)}{\sqrt{B(i,i,k)B(j,j,k)}},k=1,2,\cdots. \end{aligned} \tag{36}$$

It is clear that $\rho(i,i,k)=1$ holds for all k and i. Since all $V(i,j,k)$ are nonnegative and $\rho(i,j,k)\in[0,1]$, due to the fact that the nonnegative initial values implies that $\rho(i,j,k)$, $i,j=1,\cdots,p$ keep nonnegative all the time, it holds that

$$B(i,i,k)\leq\sum_{u,v=1}^{p}V(i,u,k)V(i,v,k)=\left[\sum_{u=1}^{p}V(i,u,k)\right]^2.$$

Then, we can construct a linear comparison system $R(k)=[r(i,j,k)]_{i,j=1}^{N}$ as follows

$$r(i,j,k+1)=\begin{cases}\dfrac{\sum_{u,v=1}^{p}V(i,u,k)V(j,v,k)r(u,v,k)}{[\sum_{u=1}^{p}V(i,u,k)]\,[\sum_{v=1}^{p}V(j,v,k)]} & i\neq j\\ 1 & i=j\end{cases}. \tag{37}$$

One can see that if with the identical nonnegative initial conditions, $r(i,j,k)\leq\rho(i,j,k)$ holds for all $i,j=1,\cdots,p$ and k. Letting $q(k)=vec(R(k))\in R^{p^2}$ with $q((i-1)N+j,k)=r(i,j,k)$, Eq. (37) has in the following vector form:

$$q(k+1)=Q(k)q(k), \tag{38}$$

where $Q(k)=[Q(s,t,k)]_{s,t=1}^{p^2}$ is defined accordingly:

$$Q((i-1)p+j,(v-1)p+u,k)=\begin{cases}\dfrac{V(i,u,k)V(j,v,k)}{[\sum_{u=1}^{p}V(i,u,k)]\,[\sum_{v=1}^{p}V(j,v,k)]} & i\neq j\\ \dfrac{1}{p} & i=j,\quad u=v\\ 0 & i=j,\quad u\neq v\end{cases}.\ \square$$

One can see that $Q(k)$ is a stochastic matrix, i.e., a nonnegative matrix with all row sums 1. One can see that every homogeneous vector $\alpha[1,1,\cdots,1]^{\top}$ for any α is a fixed point of the comparison system (38). So, this system (38) is in fact with the same form as the so-called consensus algorithm/protocol of networks of multi-agent systems (Olfati-Saber et al., 2007).

For the recurrent neuronal network, namely, W^k is constant, since $\mathcal{G}(W)$ has spanning trees and W has all diagonals positive, there exists one neuron i_0 which can access all other neurons. Consider the correlation between the self-link (i_0,i_0), namely, the components in $Q(k)$ corresponding to $q((i_0-1)p+i_0,k)$. Since $V(i,j,k)=W(i,j,k)\sigma(j,k)\geq W(i,j,k)\sigma_0$ and $W(i,i,k)\geq e$, we have

$$\begin{aligned} Q((i-1)p+j,(i-1)p+v,k) &= \frac{V(i,i,k)V(j,v,k)}{[\sum_{u=1}^{p}V(i,u,k)]\,[\sum_{v=1}^{p}V(j,v,k)]}\\ &\geq\frac{e\sigma_0}{M}W(j,v,k),\\ Q((i-1)p+j,(u-1)p+j,k) &= \frac{V(i,u,k)V(j,j,k)}{[\sum_{u=1}^{p}V(i,u,k)]\,[\sum_{v=1}^{p}V(j,v,k)]}\\ &\geq\frac{e\sigma_0}{M}W(i,u,k), \end{aligned} \tag{39}$$

for some positive constant M. Let $\delta=\frac{e\sigma_0^2}{M}\delta_0$ where $\delta_0=\min\{W(i,j):W(i,j)\neq 0\}$.

Let us consider the graph corresponding to the matrix $Q(\cdot)$: $\mathcal{G}(Q)$, which has p^2 nodes: denoted by $\{n(i,j),i,j=1,\cdots,p\}$. From the theory of stability analysis of consensus algorithm/protocol as mentioned by Olfati-Saber et al. (2007), we know that if the graph $\mathcal{G}(Q(\cdot))$ has spanning trees and the positive diagonals, then the each component of the system (38) converges to a homogeneous value. First, it is clear that in $\mathcal{G}(Q(\cdot))$, the node $n(i,j)$ has self-links for each i and j, owing to the first fact in (39) with letting $v=j$ as well as the condition that $W(i,i)>e$. Since the graph $\mathcal{G}(W)$ has spanning tree, there exists a node i_0 such that for each node l, there exist a path from i to l.

We will prove the first claim in Theorem 3.3.1 by constructing paths in the graph $\mathcal{G}(Q(\cdot))$ from $n(i_0,i_0)$ to all other node $n(k,l)$. According the condition, there exist paths from i to k and l in $\mathcal{G}(W)$, respectively. Let $i_0=k_1,k_2,\cdots,k_m=k$ and $i_0=l_0,l_1,\cdots,l_N$ be those paths. From the fact (39), one can see that there exists a δ-link in $\mathcal{G}(Q(\cdot))$ from $n(i_0,i_0)$ to $n(i_0,l_1)$. Continuing this phase, one can draw the conclusion that there exists a δ-path: $n(i_0,i_0),n(i_0,l_1),\cdots,n(i_0,l)$, from $n(i_0,i_0)$ to $n(i_0,l)$. By the same reasoning, one can see that there exists a δ-path: $n(i_0,l),n(k_1,l),\cdots,n(k,l)$, from $n(i_0,l)$ to $n(k,l)$. Therefore, there exists a δ-path from $n(i_0,i_0)$ to $n(k,l)$. Due to the arbitrariness of $n(k,l)$, one can see that their δ-graphs all have spanning trees for all time and has all positive self-links. By Olfati-Saber et al. (2007), one can conclude that $\lim_{k\to\infty}q(z,k)=\alpha$ for all z, where α is a constant, independent of the index z. Since $q((i_0-1)N+i_0,k)=1$ for all k, $\alpha=1$ holds. So, $\lim_{k\to\infty}q(k)=1$, where $1=[1,1,\cdots,1]^{\top}\in R^{p^2}$ is a column vector with all components equal to 1.

For the case of feedforward neuronal network, the proof is rather complicated. From Ineq. (39), the results by Liu et al. (2009) can lead that $q(k)$ converges to certain consensus value $\alpha 1$ for some α in the exponential p-moment sense, i.e., $E\|q(k)-\alpha 1\|^{\beta}=O(\mu^k)$ for some $\beta>1$ and $\mu\in(0,1)$. Due to $q((i-1)N+i,k)=1$ for all i and k, one can conclude that $\alpha=1$. Therefore, $q(k)$ converges to 1 almost surely.

Notice that $\rho(i,j,k)\geq r(i,j,k)$ and $\rho(i,j,k)$ can never larger than 1. Since $\rho(i,i,k)=1$ holds for all i and k, this implies that $\rho(i,j,k)$ must converge to 1. This completes the proof.

We give two remarks. First, adaptive process is rather general, including the independent identical distribution (i.i.d.) and the homogeneous Markov chain as special cases, and can even be non-stationary or non-ergodic. In those cases, Theorem 3.3.1 still works. Second, for the case that the initial values have several negative elements, if the states of correlation can be nonnegative after several iterations, under the hypotheses and conditions in the Theorem 3.3.1,

[3] Adaptive process $\{W(k),\mathcal{F}_k\}$, where $\mathcal{F}_k$ represents the σ-algebra, is defined by the condition of nondecreasing σ-algebras, i.e., $\mathcal{F}_k\subseteq\mathcal{F}_k+1$ holds for all k.

Please cite this article as: Lu, W., et al., On a Gaussian neuronal field model, NeuroImage (2010), doi:10.1016/j.neuroimage.2010.02.075

ARTICLE IN PRESS

all the correlation converges to 1 as $k\to\infty$. For instance, sufficiently small negative initial data or sufficiently large self-connection weights such that $\sum_{u,v=1}^{p} V(i,u,0)V(j,v,0)\rho(u,v,0)\geq 0$ holds for all $i,j=1,\cdots,p$.

Appendix C. Moment maps for nonlinear LIF model

In this appendix, we try to derive moment equations of neuronal spikes for general nonlinear LIF neuron models. In the literature, we have encountered many different versions of the LIF model. The most straightforward extension is possibly the nonlinear LIF model taking the following form:

$$dV = \alpha(V)dt + \beta(V)dW_t. \tag{40}$$

When $V\leq V_{th}$ and a spike is generated whenever $V=V_{th}$ from below and V is reset to V_r, where μ and σ are, in general, a function of V, and W_t is a standard Winier process (Brownian motion). Here, we consider the moments of the first passage time (FPT) from some reset potential V_r to the fixed threshold V_{th}. Let $T(V_r)$ be the random variable of the FPT from the reset potential V_r to the threshold V_{th} with $V_r\leq V_{th}$ and $M_k(V_r)=E[T(V_r)^k]$ be the k-th moment of $T(V_r)$. Based on the Fokker–Planck equation, we have the following iterative differential equations with respect to $M_k(V_r)$ (Tuckwell and Wan, 1984):

$$\frac{1}{2}\beta^2(V_r)\frac{d^2M_k(V_r)}{dV_r^2} + \alpha(V_r)\frac{dM_k(V_r)}{dV_r} = -kM_{k-1}(V)_r \tag{41}$$

with boundary conditions: $M_k(V_{th})=0$ and $M_k(V_{th}-a)=0$ for some $a>0$. Define

$$s(x) = \exp\left(-\int_0^x \frac{2\alpha(y)}{\beta^2(y)}dy\right). \tag{42}$$

We can write down a general solution of (41) as

$$M_k(V_r) = c_1\int_{V_r}^{V_{th}} s(\rho)d\rho + c_2 + \int_{V_r}^{V_{th}} d\rho\int_{V_r}^{\rho}\frac{s(z)}{s(\rho)}\left[\frac{-2kM_{k-1}(\rho)}{\beta^2(\rho)}\right]dz,$$

where $c_{1,2}$ are constants. Noting the boundary conditions, we have $c_2=0$ and

$$c_1\int_{V_{th}-a}^{V_{th}} s(\rho)d\rho + \int_{V_{th}-a}^{V_{th}} d\rho\int_{V_{th}-a}^{\rho}\frac{s(z)}{s(\rho)}\left[\frac{-2kM_{k-1}(\rho)}{\beta^2(\rho)}\right]dz = 0.$$

Letting $a\to+\infty$, we get

$$c_1 = \int_{-\infty}^{V_{th}}\frac{2kM_{k-1}(\rho)}{\beta^2(\rho)s(\rho)}d\rho,$$

which leads its solution

$$M_k(V_r) = \int_{V_r}^{V_{th}} du\int_{-\infty}^{u}\frac{s(u)}{s(v)}\frac{2kM_{k-1}(v)}{\beta^2(v)}dv. \tag{43}$$

In particular, since $M_0=1$, we have the first and second moments as

$$M_1(V_r) = \int_{V_r}^{V_{th}} du\int_{-\infty}^{u}\frac{s(u)}{s(v)}\frac{2}{\sigma^2(v)}dv$$

$$M_2(V_r) = \int_{V_r}^{V_{th}} du\int_{-\infty}^{u}\frac{s(u)}{s(v)}\frac{4M_1(v)}{\sigma^2(v)}dv.$$

Still regarding the spike trains as a renewal point process, we can derive the mean firing rate and the variance of the spike train process as:

$$\mu[\alpha,\beta] = \frac{1}{T_{\text{ref}} + M_1}$$

$$\sigma[\alpha,\beta] = \frac{\sqrt{M_2 - M_1^2}}{M_1^{3/2}},$$

which can be regarded as functionals with respect to $\alpha(\cdot)$ and $\beta(\cdot)$. Consider a general model of the network of coupled LIF neurons:

$$dV(x,t) = \alpha_{\bar{\mu}_{x,t},\bar{\sigma}_{x,t}}(V)dt + \beta_{\bar{\mu}_{x,t},\bar{\sigma}_{x,t}}(V)dW,$$

where the $\bar{\mu}_{x,t}$ and $\bar{\sigma}_{x,t}$ denote the input spike trains from the other neurons to the neuron located at x at time t, the symbols $\alpha_{\bar{\mu}_{x,t},\bar{\sigma}x,t}(\cdot)$ and $\beta_{\bar{\mu}_{x,t}\bar{\sigma}x,t}(\cdot)$ show the dependence of the functions with respect to the input spikes. Thus, we can derive the moment equations for the random field with respect to the spikes trains:

$$\tau\frac{d\mu(x,t)}{dt} = -\mu(x,t) + \mu\left[\alpha_{\bar{\mu}_{x,t},\bar{\sigma}_{x,t}},\beta_{\bar{\mu}_{x,t},\bar{\sigma}_{x,t}}\right]$$

$$\tau\frac{d\sigma(x,t)}{dt} = -\sigma(x,t) + \sigma\left[\alpha_{\bar{\mu}_{x,t},\bar{\sigma}_{x,t}},\beta_{\bar{\mu}_{x,t},\bar{\sigma}_{x,t}}\right].$$

Furthermore, based on the iterative Eq. (43) and the renewal process theory, we can derive the moment equations for any order moments of the ISI and the spike trains. In addition, the coefficients of correlation can also be derived by the linear perturbation theory similar to as done by Gammaitoni et al. (1998), which is omitted here.

As a special case, the linear LIF model, we have $\mu(x)=-Lx+\bar{\mu}$ and $\sigma(x)=\bar{\sigma}$. Then, after complicated algebras, Eq. (43) yields the mean and variance of the FTP (or ISI) as follows:

$$E(T) = 2L\int_{\frac{V_rL-\mu}{\sigma\sqrt{L}}}^{\frac{V_{th}L-\mu}{\sigma\sqrt{L}}}\exp\left(x^2\right)\int_{-\infty}^{x}\exp\left(-y^2\right)dydx$$

$$\text{Var}(T) = \frac{8}{L^2}\int_{\frac{V_rL-\mu}{\sigma\sqrt{L}}}^{\frac{V_{th}L-\mu}{\sigma\sqrt{L}}}\exp\left(u^2\right)\int_{-\infty}^{u}\exp\left(-v^2\right)D_-^2(v)dvdu,$$

which is used in the main part of this paper.

References

Amari, S., 1975. Homogeneous nets of neuron-like elements. Biol. Cybern. 17, 211–220.
Amari, S., 1977. Dynamics of pattern formation in lateral-inhibition type neural fields. Biol. Cybern. 27, 77–87.
Amari, S., Nakahara, H., 2006. Correlation and independence in the neural code. Neural Comput. 18, 1259–1267.
Averbeck, B.B., Latham, P.E., Pouget, A., 2006. Neural correlations, population codes and computation. Nat. Rev. Neurosci. 7 (358–366), 2006.
Breakspear, M., Terry, J., Friston, K.J., 2003. Modulation of excitatory synaptic coupling facilitates synchronization and complex dynamics in a biophysical model of neuronal dynamics. Netw. Comput. Neural Syst. 14, 703–732.
Brette, R., Gerstner, W., 2005. Adaptive exponential integrate-and-fire model as an effective description of neuronal activity. J. Neurophysiol. 94, 3637–3642.
Brown, D., Feng, J.F., Ferrick, S., 1999. Variability of firing of Hodgkin–Huxley and FitzHuge–Nagumo neurons with stochastic input. Phys. Rev. Lett. 82, 4731–4734.
Brunel, N., Wang, X., 2001. Effects of neuromodulation in a cortical network model of object working memory dominated by recurrent inhibition. J. Comput. Neurosci. 11, 63–85.
Buice, M.A., Chow, C.C., 2007. Correlations, fluctuations, and stability of a finite-size network of coupled oscillators. Phys. Rev. E 76, 03111.
Burak, Y., Lewallen, S., Simpolinsky, H., 2009. Neural Comput. 21, 2269–2308.
Cai, D., et al., 2004. An efficient kinetic representation of fluctuation-driven neuronal network with application to simple and complex cells in visual cortex. Proc. Natl. Acad. Sci. 101, 7757–7762.

Please cite this article as: Lu, W., et al., On a Gaussian neuronal field model, NeuroImage (2010), doi:10.1016/j.neuroimage.2010.02.075

Caronell, F., Worsley, K.J., Trujillo-Barreto, N., Sotero, R.C., 2009. Random fields — union intersection tests for detecting functional connectivity in EEG/MEG imaging. Hum. Brain Mapp. doi:10.1002/hbm.20685.
Cateau, H., Reyes, A.D., 2006. Relation between single neuron and population spiking statistics and effects on network activity. Phys. Rev. Lett. 96, 058101.
Cox, P.R., Lewis, P.A.W., 1996. The Statistical Analysis of Series of Events. Latimer Trend & Co., Whitstable.
Dayan, P., Abbott, L., 2002. Theoretical Neuroscience: Computational and Mathematical Modelling of Neural Systems. MIT Press, Boston.
De La Rocha, J., Doiron, J.B., Shea-Brown, E., Josic, K., Reyes, A., 2007. Correlation between neural spike trains increases with firing rate. Nature 448, 802–806.
Deco, G., Rolls, E.T., 2003. Attention and working memory: a dynamical model of neuronal activity in the prefrontal cortex. Eur. J. Neurosci. 18, 2374–2390.
Deco, G., Jirsa, V.K., Robinson, P.A., Breakspear, M., Friston, K.J., 2008. The dynamic brain: from spiking neurons to neural masses and cortical fields. PLoS Comp. Biol. 4, e1000092. doi:10.1371/journal.pcbi.1000092.
Destexhe, A., Contreras, D., 2006. Neuronal computations with stochastic network states. Science 314, 85–90.
Diesmann, M., Gewaltig, M.-O., Aertsen, A., 1999. Stable propagation of synchronous spiking in cortical neural networks. Nature 402, 529–533.
Erlhagen, W., Schöner, G., 2002. Dynamic field theory of movement preparation. Psych. Rev. 109, 545–572.
Ermentrout, G., Kleinfeld, D., 2001. Traveling electrical waves in cortex: insights from phase dynamics and speculation on a computational role. Neuron 29, 33–44.
Feng, J.F., 2003. Computational Neuroscience — a Comprehensive Approach. FL: Chapman and Hall/CRC Press, London/Boca Raton.
Feng, J.F., Brown, D., 1999. Coefficient of variation greater than 0.5 how and when? Biol. Cybern. 80 (5), 291–297.
Feng, J.F., Brown, D., 2000. Impact of correlated inputs on the output of the integrate-and-fire models. Neural Comput. 12, 671–692.
Feng, J.F., Tuckwell, H.C., 2003. Optimal control of neuronal activity. Phys. Rev. Lett. 91, 018101.
Feng, J.F., Tartaglia, G., Tirozzi, B., 2004. A note on the minimum variance theory and beyond. J. Phys. A 37, 4685–4700.
Feng, J.F., Deng, Y., Rossoni, E., 2007. Dynamics of moment neuronal networks. Phys. Rev. E 73, 041906.
Firston, K.J., Holmes, A.P., Worsley, K.J., Poline, J.-P., Frith, C.D., Frackowiak, R.S.J., 1995. Statistical parametric maps in functional imaging; A general linear approach. Hum. Brain Mapp. 2, 189–210.
Fourcaud, N., Brunel, N., 2002. Dynamics of the firing probability of noisy integrate-and-fire neurons. Neural Comput. 14, 2057–2110.
Fourcaud, N., Hansel, D., van Vreeswijk, C., Brunel, N., 2003. How spike generation mechanisms determine the neuronal response to fluctuating inputs. J. Neurosci. 23, 11628–11640.
Freidlin, M.I., Wentzell, A.D., 1998. Random perturbations of dynamical systems, Grundlehren der Mathematischen Wissenschaften [Fundamental Principles of Mathematical Sciences] 260, Second ed. Springer-Verlag, New York, p. xii+430.
Friston, K.J., et al., 1994. Assessing the significance of focal activations using their spatial extent. Hum. Brain Mapp. 1, 210–220.
Gammaitoni, L., et al., 1998. Stochastic resonance. Rev. Mod. Phys. 71, 233–287.
Gerstner, W., Kistler, W., 2002. Spiking Neuron Models Single Neurons, Populations, Plasticity. Cambridge University Press, Cambridge.
Griffith, J.S., 1963. A field theory of neural nets: I. Derivation of field equations. Bull. Math. Biophys. 25, 111–120.
Griffith, J.S., 1965. A field theory of neural nets: II. Properties of the field equations. Bull. Math. Biophys. 27, 187–195.
Harrison, L.M., David, O., Friston, K.J., 2005. Stochastic models of neuronal dynamics. Philos. Trans. R. Soc. B 360, 1075–1091.
Hayasaka, S., Peiffer, A.M., Hugenschmidt, C.E., Laurienti, P.J., 2007. Power and sample size calculation for neuroimaging studies by non-central random field theory. NeuroImage 37, 721–730.
Hildebrand, E.J., et al., 2007. Kinetic theory of coupled oscillators. Phys. Rev. Lett. 98, 054101.
Hodgkin, A., Huxley, A., 1952. A quantitative description of membrane current and its application to conduction and excitation in nerve. J. Physiol. 117, 500–544.
Humter, J.J., 1974. Renewal theory in two dimensions: asymptotic results. Adv. Appl. Probab. 6, 546–562.
Jirsa, V.K., 2004. Connectivity and dynamics of neural information processing. Neuroinformatics 2, 183–204.
Kendrick, K.M., Zhan, Y., Fischer, H., Nicol, A.U., Zhang, X.J., Feng, J.F., 2009. Learning alters theta-nested gamma oscillations in inferotemporal cortex. Nature Precedings http://hdl.handle.net/10101/npre.2009.3151.2.
Kovačič, G., et al., 2009. Fokker–Planck description of conductance-based integrate-and-fire neuronal networks. Phys. Rev. Lett. 80, 021904.
Lapicque, L., 1907. Recherches quantitatives sur lexcitation electrique des nerfs traitee comme une polarization. J. Physiol. Pathol. Gen. 9, 620–635.
Leng, G., Brown, C.H., Bull, P.M., Brown, D., Scullion, S., Currie, J., Blackburn-Munro, R.E., Feng, J., Onaka, T., Verbalis, J.G., Russell, J.A., Ludwig, M., 2001. Responses of magnocellular neurons to osmotic stimulation involves coactivation of excitatory and inhibitory input: an experimental and theoretical analysis. J. Neurosci. 21, 6967–6977.
Lindner, B., Doiron, B., Longtin, A., 2005. Theory of oscillatory firing induced by spatially correlated noise and delayed inhibitory feedback. Phys. Rev. E 72, 061919.
Liu, B., Lu, W.L., Chen, T.P., 2009. Reaching L_p consensus in a network of multiagents with stochastically switching topologies. 48th IEEE Conf. Decision Control, Shanghai, pp. 2670–2675. doi:10.1109/CDC.2009.5399996.
Ly, C., Tranchina, D., 2009. Neural Comput. 21, 360–396.
Marreiros, A.C., Kiebel, S.J., Daunizeau, J., Harrison, L.M., Friston, K.J., 2009. Population dynamics under Laplace assumption. NeuroImage 44, 701–714.
Mehring, C., Hehl, U., Kubo, M., Diesmann, M., Aertsen, A., 2003. Activity dynamics and propagation of synchronous spiking in locally connected random networks. Biol. Cybern. 88, 395–408.
Memmesheimer, R.M., Timme, M., 2006. Designing the dynamics of spiking neural networks. Phys. Rev. Lett. 97, 188101.
Meyer, C., van Vreeswijk, C., 2002. Temporal correlations in stochastic networks of spiking neurons. Neural Comp. 10, 1321–1372.
Miles, R., Traub, R., Wong, R., 1995. Spread of synchronous firing in longitudinal slices from the CA3 region of hippocampus. J. Neurophysiol. 60, 1481–1496.
Niebur, E., Hsiao, S.S., Johnson, K.O., 2002. Synchrony: a neuronal mechanism for attentional selection? Curr. Opin. Neurobiol. 12, 190–194.
Nunez, P.L., 1974. The brain wave equation: a model for EEG. Math. Biosci. 21, 279–297.
Olfati-Saber, R., Fax, J.A., Murray, R.M., 2007. Consensus and cooperation in networked multi-agent systems. Proc. IEEE 95 (1), 215–233.
Pantazis, D., Nichols, T.E., Baillet, S., Leahy, R.M., 2005. A comparison of random field theory and permutation methods for the statistical analysis of MEG data. NeuroImage 25, 383–394.
Pospischil, M., et al., 2009. Characterizing neuronal activity by describing the membrane potential as a stochastic process. J. Physiol. 103, 98–106.
Reyes, A.D., 2003. Synchrony-dependent propagation of firing rate in iteratively constructed networks in vitro. Nat. Neurosci. 6, 593.
Rieke, F., Warland, D., Steveninck, R., 1997. Spikes: Exploring the Neural Code. MIT Press, Cambridge, MA/London.
Romo, R., Hernandez, A., Zainos, A., 2004. Neuronal correlates of a perceptual decision in ventral premotor cortex. Neuron 41, 165–173.
Sarnthein, J., Petsche, H., Rappelsberger, P., Shaw, G.L., von Stein, A., 1998. Synchronization between prefrontal and posterior association cortex during human working memory. Proc. Natl. Acad. Sci. U. S. A. 95, 7092–7096.
Sporns, O., 2003. Complex neural dynamics. In: Jirsa, V.K., Kelso, J.A.S. (Eds.), Coordination Dynamics: Issues and Trends. Springer, Berlin.
Svensén, M., Kruggel, F., von Cramon, Y., 2000. Probabilistic modelling of single-trial fMRI data. IEEE Trans. Med. Imaging 19, 25–35.
Tuckwell, H.C., 1988. Introduction to Theoretical Neurobiology. Cambridge Univ. Press, Cambridge, UK.
Tuckwell, H.C., Wan, F.Y.M., 1984. First-passage time of Markov process to moving barriers. J. Appl. Prob. 21, 695–709.
Vanmarke, R., 1983. Random Fields: Analysis and Synthesis. The MIT Press, Cambridge, Massachusetts.
Varela, F., Lachaux, J.-P., Rodriguez, E., Martinerie, J., 2001. The brainweb: phase synchronization and large-scale integration. Nat. Rev. Neurosci. 2, 229–239.
Wang, Y., Rajapakse, J.C., 2006. Contextual modelling of functional MR images with conditional random fields. IEEE Trans. Med. Imaging 32, 804–812.
Wilson, H.R., Cowan, J.D., 1972. Excitatory and inhibitory interactions in localized populations of model neurons. Biophys. J. 12, 1–24.
Wilson, H.R., Cowan, J.D., 1973. A mathematical theory of the functional dynamics of cortical and thalamic nervous tissue. Kybernetik 13, 55–80.
Wu, J.Y., Guan, L., Tsau, Y., 1999. Propagating activation during oscillations and evoked responses in neocortical slices. J. Neurosci. 19, 5005–5015.
Zhang, X.J., You, G.Q., Chen, T.P., Feng, J.F., 2009. Maximum likelihood decoding of neuronal inputs from inter-spike interval distribution. Neural Comput. 21 (11), 3079–3105.

Please cite this article as: Lu, W., et al., On a Gaussian neuronal field model, NeuroImage (2010), doi:10.1016/j.neuroimage.2010.02.075